TITLE: Male-specific features are reduced in *Mecp2*-null mice: analyses of vasopressinergic innervation, pheromone production and social behaviour

AUTHORS: Elena Martínez-Rodríguez[1a], Ana Martín-Sánchez[1a,b], Emre Kul[2], Aparajita Bose[2c], Francisco José Martínez-Martínez[1], Oliver Stork[2], Fernando Martínez-García[1], Enrique Lanuza[1], Mónica Santos[2,3]*, Carmen Agustín-Pavón[1]*

1 Unitat Mixta d'Investigació Neuroanatomia Funcional, Departament de Biologia Cel·lular, Funcional i Antropologia Física, Universitat de València, and Unitat Predepartamental de Medicina, Universitat Jaume I de Castelló (Spain)

2 Department of Genetics and Molecular Neurobiology, Institute of Biology, and Center for Behavioral Sciences, Otto-von-Guericke University, Magdeburg (Germany)

3 CNC - Center for Neuroscience and Cell Biology, University of Coimbra (Portugal).

a These authors contributed equally to the work.

b Current address: Neurobiology of Behaviour Research Group (GReNeC-NeuroBio), Department of Experimental and Health Sciences, Universitat Pompeu Fabra, Barcelona, Spain; Neuroscience Research Program, IMIM-Hospital del Mar Research Institute, Barcelona (Spain).

c Current address: Neurologie, Ammerland-Klinik GmbH

*__Correspondence__:

Carmen Agustín-Pavón

ORCID ID: 0000-0002-6725-6954

Departament de Biologia Cel·lular, Biologia Funcional i Antropologia Física,

Universitat de València

Av. Vicent Andrés Estellés, s/n

46100 Burjassot, Spain

Email: pavon@uv.es

Mónica Santos

ORCID ID: 0000-0003-3229-8270CNC - Center for Neuroscience and Cell Biology

University of Coimbra

Rua Larga, Faculdade de Medicina, pólo I, 2º andar

3004-504, Coimbra, Portugal

Email: mjpsantos@cnc.uc.pt

ACKNOWLEDGEMENTS

Authors are indebted to Chelsie Villanueva-Hayes for technical support in the acquisition of pilot data and Dr. Adoración Hernández-Martínez for providing a supplementary figure. Funded by the Spanish Ministry of Economy and Competitiveness (BFU2016-77691-C2-1-P) to FMG, EL and CAP; Conselleria d'Educació, Investigació, Cultura i Esport (PROMETEO/2016/076) and Universitat Jaume I (UJI-B2016-45) to FMG; E-Rare-2 JTC 2012 and E-Rare-2 JTC 2014 by the German Federal Ministry of Education and Research (BMBF) [01GM1302 to M.S., 01GM1505 to O.S.]; Bial Foundation, Grants for Scientific Research, 85/18 to M.S.; and *Ayudas FinRett 2019 para la Investigación del Síndrome de Rett* to CAP.

ABSTRACT

Deficits in arginine-vasopressin (AVP) and oxytocin (OT), two neuropeptides closely implicated in the modulation of social behaviours, have been reported in some early developmental disorders and autism spectrum disorders. Mutations in the X-linked methyl CpG binding protein 2 (*MECP2*) gene are associated to Rett syndrome and other neuropsychiatric conditions. Thus, we first analysed AVP and OT expression in the brain of *Mecp2*-mutant mice by immunohistochemistry. Our results reveal no significant differences in these systems in young adult *Mecp2*-heterozygous females, as compared to WT littermates. By contrast, we found a significant reduction in the sexually dimorphic, testosterone-dependent, vasopressinergic innervation in several nuclei of the social brain network and of oxytocinergic innervation in the lateral habenula of *Mecp2*-null males, as compared to WT littermates. Analysis of urinary production of pheromones show that *Mecp2*-null males lack the testosterone-dependent pheromone *darcin*, strongly suggesting low levels of androgens in these males. In addition, resident-intruder tests revealed lack of aggressive behaviour in *Mecp2*-null males and decreased chemoinvestigation of the intruder. By contrast, *Mecp2*-null males exhibited enhanced social approach, as compared to WT animals, in a 3-chamber social interaction test. In summary, *Mecp2*-null males, which display internal testicles, display a significant reduction of some male-specific features such as vasopressinergic innervation within the social brain network, male pheromone production and aggressive behaviour. Thus, atypical social behaviours in *Mecp2*-null males may be caused, at least in part, by the effect of lack of MeCP2 over sexual differentiation.

Keywords: Aggression; Autism Spectrum Disorders; Methyl-CpG binding protein 2; Nonapeptides; Rett syndrome; Social behaviour

DECLARATIONS

Funding

Funded by the Spanish Ministry of Economy and Competitiveness (BFU2016-77691-C2-1-P) to FMG, EL and CAP; Conselleria d'Educació, Investigació, Cultura i Esport (PROMETEO/2016/076) and Universitat Jaume I (UJI-B2016-45) to FMG; E-Rare-2 JTC 2012 and E-Rare-2 JTC 2014 by the German Federal Ministry of Education and Research (BMBF) [01GM1302 to M.S., 01GM1505 to O.S.]; Bial Foundation, Grants for Scientific Research, 85/18 to M.S.; and Ayudas FinRett 2019 para la Investigación del Síndrome de Rett to CAP.

Competing interests

The authors declare no competing interests.

Authors' contributions

CAP, MS, FMG and EL designed research. EMR, AMS, EK, AB, FJMM and MS performed research. EMR, AMS, CAP and MS analysed data. EMR, AMS, CAP and MS wrote the paper. EL, FMG and OS discussed the data and the draft of the manuscript. OS provided mice. All authors read and approved the final version of the manuscript. The authors declare no competing interests.

Ethics approval

All the procedures were carried out in strict accordance with the EU directive 2010/63/EU. The protocols were approved by the local veterinary office of the University Otto-von-Guericke and the Animal Experimentation Ethics Committee of the University of Valencia, Protocol 2019/VSC/PEA/0027.

Consent to participate/ Consent for publication

Not applicable.

Availability of data and materials

The datasets used and/or analysed during the current study are available from the corresponding author on reasonable request.

ABBREVIATIONS

AC/ADP: nucleus of the anterior commissure / anterodorsal preoptic nucleus region

AcbC: nucleus accumbens, core

AcbSh: nucleus accumbens, shell

BST: bed nucleus of the stria terminalis

BSTMPI: bed nucleus of the stria terminalis, medial division, posterointermediate part

Ce: central amygdaloid nucleus

dEn: dorsal endopiriform cortex

dlPAG: dorsolateral periaqueductal grey

DMH: dorsomedial hypothalamic nucleus

DR: dorsal raphe nucleus

LHb: lateral habenular nucleus

LS: lateral septum

Me: medial amygdaloid nucleus

MeA: medial amygdaloid nucleus, anterior part

MePD: medial amygdaloid nucleus, posterodorsal part

Opt: optic tract

Pa: paraventricular hypothalamic nucleus

Pe: periventricular hypothalamic nucleus

SCh: suprachiasmatic nucleus

SON: supraoptic nucleus

SOR: retroquiasmatic part of the supraoptic nucleus

St: striatum

vHip: ventral hippocampus

vlPAG: ventrolateral periaqueductal grey

vmStP: ventromedial striatopallidum

INTRODUCTION

Arginine-vasopressin (AVP) and oxytocin (OT) are two related nonapeptides mainly synthesized in the hypothalamic paraventricular (Pa) and supraoptic nuclei (SON). In addition, AVP is present in the suprachiasmatic nucleus (SCh), and AVP-containing neurons in the bed nucleus of the stria terminalis (BST) and medial amygdala (Me), display a marked sexual dimorphism in favour of males (Rood et al. 2013; Otero-Garcia et al. 2014, 2016). Central projections of the nonapeptide-synthesising groups to brain nodes of the social brain network possess relevant roles in the control of social, sexual and parental behaviours in mammals (Goodson 2008). Interestingly some of the target regions of AVP neurons, such as the ventral lateral septum (LS), medioventral striato-pallidum (vmStP), posterodorsal medial amygdala (MePD) or lateral habenula (LHb) display significantly higher density of AVP-immunoreactive (ir) fibres in males than in females (Otero-Garcia et al. 2014).

This sexually-dimorphic AVP innervation is dependent on testosterone (Rood et al. 2013; Otero-Garcia et al. 2014), which aromatized to estradiol acts on estradiol receptor α (ERα) (Scordalakes and Rissman 2004). In turn, transcriptional regulators such as the methyl CpG-binding protein 2 (MeCP2) are involved in the regulation of both AVP and ERα (Murgatroyd et al. 2009; Westberry et al. 2010; Forbes-Lorman et al. 2012), suggesting a complex interplay between gonadal hormones and epigenetics. This interplay would contribute to the shaping and functioning of the social brain nuclei (Newman 1999), key for the development and expression of social behaviour (Auger et al. 2011; Romano et al. 2016).

Mutations in the *MECP2* gene, located on the Xq28 chromosome, underlie 95% of the classic cases of Rett syndrome [RTT, OMIM #312750; (Zoghbi et al. 1999)], a rare neurodevelopmental disorder first described by Andreas Rett in 1966 [(Rett 2016) translation of the original article (Rett 1966)]. Although considered as a rare disease, which affects 1 in 10.000 girls, RTT represents the second cause of intellectual disability of genetic origin in females (Christodoulou 2001). Girls affected with RTT show normal development until the age of 6 to 18 months, when they start to manifest the typical symptomatology such as loss of previously acquired speech and motor abilities, breathing abnormalities, stereotypic hand movements, seizures, intellectual disability, and autistic features (Hagberg 2002). In the case of boys, they usually die from severe neonatal encephalopathy before the first year of life [reviewed in (Santos et al. 2009)]. By contrast, boys with *MECP2*-duplication syndrome display intellectual disability and autism, whereas girls are either asymptomatic carriers or display some neuropsychiatric symptoms (Ramocki et al. 2010). The wide variety

of neurological and neuropsychiatric symptoms caused by either lack or excess of MeCP2 protein is related to its important expression in the mature neurons of the central nervous system (LaSalle et al. 2001).

Deficits in vasopressinergic (AVP-ergic) and oxytocinergic (OT-ergic) systems have been involved in neurodevelopmental, autistic and psychiatric disorders in both humans and rodents (Waterhouse et al. 1996; Modahl et al. 1998; Winslow and Insel 2004; Domes et al. 2007; Lukas and Neumann 2013; Miller et al. 2013; Francis et al. 2014; Menon et al. 2018; Freeman et al. 2018). However, AVP-ergic and OT-ergic systems have not been analysed in mouse models of *MECP2*-related syndromes.

On this basis, our first aim was to analyse the consequences of MeCP2 deficit on AVP and OT distribution in the brain of young adult male and female mice, using an established *Mecp2*-mutant mouse model, the *Mecp2*$^{tm1.1Bird}$ (Guy et al. 2001). In this strain, hemizygous males (*Mecp2*-null) are infertile, so the breeding pairs are established with *Mecp2*-heterozygous (*Mecp2*-het) females paired to WT males. This impedes the production of *Mecp2*-null females in this strain, and hence, in this study, we compare males and females separately, as we did in a previous study (Martínez-Rodríguez et al. 2019).

Given that our results showed that lack of MeCP2 affects mainly the testosterone-dependent AVP-ergic innervation in male mice, we next analysed the production of masculine urinary pheromones, also dependent on testosterone levels, in the *Mecp2*-null males. Finally, since gonadal steroids influence agonistic and social behaviour, we analysed the behavioural profile of *Mecp2*-null males in the resident-intruder and in the three-chamber social interaction tests.

MATERIAL AND METHODS

Mice

For this study, we used a total of 50 *Mecp2*-mutant mice (Guy et al. 2001) and 82 of their wild-type (WT) siblings as controls, purchased from The Jackson Laboratory (B6.129(C)-*Mecp2*$^{tm1.1Bird}$). Of those, we used 23 mice for the analysis of AVP and OT distribution (WT females, n=5; WT males, n=7; *Mecp2*-het females, n= 6; *Mecp2*-null males, n=5). We obtained urine from 8 males to study the presence of Major Urinary Proteins (MUPs), pheromones released in the urine (WT male, n=4; *Mecp2*-null males, n=4). Finally, 45 male mice were used for the resident intruder test (RI-test) for intermale aggression (male WT, n=32; male *Mecp2*-null, n=13), 16 were used for the habituation-dishabituation test of olfactory function

(male WT, n=7; *Mecp2*-null male, n=9), and 40 for the social preference test (male WT, n=27; *Mecp2*-null male, n=13). All animals were 8 weeks old when tested.

Mice were housed in groups of 2-5 animals in standard laboratory cages with controlled humidity and temperature (22ºC), a 12:12-h light/dark cycle, and water and food available *ad libitum*. All the procedures were carried out in strict accordance with the EU directive 2010/63/EU. The protocols were approved by the local veterinary office of the University Otto-von-Guericke and the Animal Experimentation Ethics Committee of the University of Valencia.

Genotyping

For genotyping, we applied the protocol supplied by the Jackson Laboratory for this strain after the extraction of the DNA from the tail tips of the mice at weaning.

Histology

Animals for anatomical studies were deeply anaesthetized using a mixture of ketamine (75 mg/Kg) and medetomidine (1 mg/Kg) and transcardially perfused with saline solution followed by 4% formaldehyde in 0.1M phosphate buffer pH 7.4. Brains were carefully removed from the skull, postfixed in the same fixative for 4 h and placed into 30% sucrose (in 0.01M phosphate buffered saline, pH 7.6, PBS) until they sank. The brains were then frozen and cut in five series of 40-µm-thick coronal sections with a freezing microtome. Free-floating sections were stored in the freezer in phosphate buffered 30% sucrose (0.1 M pH 7.4) until they were used.

Double immunofluorescence for arginine-vasopressin and oxytocin

We employed combined immunofluorescence for simultaneous immunolabelling of AVP and OT following Otero-García et al., (2016). For this experiment we used one out of five parallel series obtained of mice sacrificed at the age of 8 weeks (female WT, n=6; male WT, n=7; *Mecp2*-het female, n=5; *Mecp2*-null male, n=5).

Sections were incubated sequentially in: (i) 1% sodium borohydride in TRIS buffered (TB) saline (TBS, 0.9% NaCl in TB) at room temperature (RT, approximately 25ºC) for 30 minutes (min); (ii) 0.05M TBS pH 7.6 with 0.3% Triton X-100, and 4% normal goat serum (NGS) at RT for 1 hour. (iii) Next, sections were incubated with TBS with 0.2% Triton X-100, 4% NGS for 48h at 4ºC with the following antibodies: rabbit anti-vasopressin IgG (1:2500; Millipore, AB1565) and mouse anti-oxytocin, monoclonal IgG (1:200;

Dr. Harold Gainer, NIH, PS38). (iv) After incubation with primary antibodies, sections were incubated with fluorescent-labelled secondary antibodies for 90 min at RT in TBS with 0.2% Triton X-100: Alexa Fluor 488-conjugated Goat anti-rabbit IgG (1:250; Jackson ImmunoResearch, 111-545- 003) and Rhodamine Red X-conjugated goat anti-mouse IgG (1:250; Invitrogen R6393). Between each step, sections were washed in TBS (except between step ii and iii). To reveal the cytoarchitecture of the brain in the same sections, prior to mounting, sections were counterstained in DAPI for 45 seconds (4',6-diamino- 2-fenilindol, 600nM) at RT. Sections were finally rinsed thoroughly in TB, mounted onto gelatinized slides and cover-slipped with fluorescence mounting medium (Dako, Glosrup, Denmark). Immunofluorescent staining of the samples to be directly compared (i.e. WT males *vs Mecp2*-null and WT females *vs Mecp2*-het) were performed at the same time, and all the material was processed by the same experimenter.

Permanent arginine-vasopressin immunohistochemistry with NADPH-diaphorase staining

We performed a permanent immunostaining for AVP combined with NADPH-diaphorase histochemistry in one of the five parallel sets of 12 males used above (male WT, n=7; *Mecp2*-null, n=5) as in Otero-Garcia et al., (2014). For AVP immunostaining, sections were incubated sequentially in: (i) 1% H_2O_2 in 0.05M TBS pH 7.6 for 30 min at RT for endogenous peroxidase inactivation; (ii) blocking solution, 0.05M TBS pH 7.6 with 0.3% Triton X-100 and 2% NGS; (iii) primary antibody (1:10000, rabbit anti-vasopressin IgG, Chemicon, AB1565) overnight at 4 ºC; (iv) diluted biotinylated secondary antibody (1:200, goat anti-rabbit IgG, Vector Labs, BA-1000) in TBS for 90 min at RT; (v) avidin–biotin-peroxidase complex (ABC Elite kit; Vector Labs, PK-6200) in TBS for 90 min at RT. Between each step, sections were washed in TBS (3x10 min). After ABC incubation, sections were rinsed in TBS (3x10min) and TRIS buffer (TB) 0.05 M, pH 8 (3x10min). The histochemical detection of the resulting peroxidase activity was performed by incubation in 0.003% H_2O_2 and 0.025% 3,3- diaminobenzidine (Sigma) in TB for about 17 min. See Supplementary information for NADPH-diaphorase histochemistry. The sections were finally rinsed thoroughly in TB, mounted onto gelatinized slides, dehydrated in ethanol, cleared with xylene and coverslipped with Entellan. Immunostaining of all the samples was performed at the same time by the same experimenter.

Analysis and quantification

An experimenter blind to genotype and sex of mice took pictures of both hemispheres of previously selected levels of Bregma (following Paxinos and Franklin, (2012); Table 1) in several brain nuclei in which either

AVP-ergic or OT-ergic innervation have been previously demonstrated in the brain of mice (Otero-Garcia et al. 2014; Otero-García et al. 2015). Pictures were taken with a digital Leica DFC495 camera attached to a microscope equipped with both conventional light and fluorescent lamps (Leica Leitz DMRB) and software LAS v4.3. We adjusted the most accurate conditions of exposition, gamma and saturation for each brain region. Pictures from both genotypes were taken under the same scan settings. Because some nuclei are heterogeneous in the density of AVP-immunoreactive (AVP-ir) and OT-ir along the rostro-caudal axis, extra levels of Bregma we selected for those, and we calculated the average density of AVP-ir and OT-ir cells for each nucleus. Pictures were obtained by using the green channel for Alexa Fluor 488 (AVP) and then changing to the red channel for Red Rhodamine-X (OT). Both images were taken at exactly the same location when co-localization analysis was required. All the subsequent steps were performed using ImageJ free software (NIH).

Quantification of AVP and OT cells: single and double staining

AVP-ir and OT-ir somata were analysed in different brain areas at previously selected Bregma levels (see Table 1). Those nuclei include the posterointermediate part of the medial division of the bed nucleus of the stria terminalis (BSTMPI) and the anterior and posterodorsal parts of the medial amygdaloid nucleus (MeA, MePD). We also analysed AVP-ir and OT-ir cells in the hypothalamic region between the anterodorsal preoptic nucleus and the nucleus of the anterior commissure (AC/ADP), as well as other hypothalamic nuclei such as Pa, SCh, SON, and the retrochisamatic region of the supraoptic nucleus (SOR). An observer blind to the experimental conditions took pictures from both hemispheres at specific objective magnification and counted manually the number of AVP-ergic and OT-ergic cells with the multipoint plugin of the ImageJ software. We also analysed co-localization of AVP and OT in the AC/ADP and Pa, using ImageJ software.

Analysis and quantification of AVP and OT immunoreactive terminal fields

AVP-ergic and OT-ergic innervation was analysed in target regions following the protocol described in (Menon et al. 2018): we draw a Grid with the plugin of the ImageJ and counted the number of crossings of the fibres with the grid bars with the multi-point tool of the Image J. In the case of the AVPergic fibres in the LHb, due to intricate labelling found, we counted the total number of squares containing labelled puncta.

Urine collection and analysis

Urine from 4 WT and 4 *Mecp2*-null males was collected by gently pressing the animal bladder manually, holding the animal over a Petri dish. We performed a mass separation of urinary proteins using 15% sodium dodecyl sulphate-polyacrylamide gel electrophoresis (SDS-PAGE) (Lanuza et al. 2014). First, we diluted the urine samples 1:1 with 20 mM Tris-HCL pH=8, 5% SDS, 10% mercaptoethanol, 2 mM EDTA and 0.05% bromophenol blue. Samples were vortexed, boiled for 5 min and centrifuged for 5 min at 10.000 rpm. Male urine was then further diluted 1:3 in 10 mM Tris-HCL pH=8, 2.5% SDS, 5% mercaptoethanol, 1mM EDTA and 0.05% of bromophenol blue.

We loaded 50 µg of total protein from the urine samples in a 15% SDS-PAGE and run at 200 V. Following electrophoresis, protein bands were visualized using PhastGel Blue (0.1%) solution at 50 ºC and differentiated in a solution of Coomassie brilliant.

Behavioural testing and analysis

All behavioural tests were performed between 10 am and 5 pm.

Resident-intruder

Animals were isolated in their home-cages for at least 1 week with no bedding changes. On the day of testing, an intruder male mouse (same strain WT or *Mecp2*-null male of 2-4 months old) was introduced in the home-cage of the test animal and the behaviour was registered for 5 min. After 1 week, the test was repeated, but now with the test animal as intruder.

An observer blind to the experimental conditions manually scored several behavioural parameters using the plugging *event recorder* of SMART 2.5 (Panlab, Barcelona, Spain). The parameters were number and total time in seconds of attack from resident to intruder, time that the resident spent investigating the intruder (sniffing the face, body or anogenital zone), number of times that the resident chased the intruder, number of times that the resident escaped from the intruder, and time spent by the resident self-grooming.

Habituation-dishabituation

WT and *Mecp2*-null mice were placed in a new cage with fresh bedding for 3 min for habituation in the experimental room. Afterwards, we presented a clean cotton bud soaked with 10µl water to the mouse three times for 1 min, with a 30 seconds gap in between. This procedure was followed with rose (1:1000 dilution) and urine (collected from C57Bl/6J animals) odour presentations. For the analysis, we registered the time animals spent sniffing the cotton bud.

Three-chamber social preference interaction test

The test consisted of 3 phases. (i) During the habituation phase, mice were put in the arena with the 2 stimulus chambers empty and allowed to freely explore for 5 min. (ii) To test for social preference, a stimulus mouse (stranger 1) confined inside one wire-mesh cylinder was introduced in one of the stimulus chambers (counterbalanced). The second cylinder was left empty in the opposite chamber and the test mouse was placed in the arena and allowed to explore for 5 min. (iii) One hour after the social preference test, animals were tested for social recognition in a 5 min session. During this stage, a second stimulus mouse (stranger 2) was confined to the previously empty cylinder, while the familiar one (stranger 1) remained in its cylinder. Stranger 1 and Stranger 2 animals were 2-4 WT males of the C57Bl6/J strain.

Behaviour was monitored automatically using a video tracking system (ANYMAZE). We recorded and analysed exploration for the familiar or the new subject, defined as the orientation of the nose towards the cylinder at a distance ≤ 2 cm. Sociability was measured as the time spent close to each cylinder (stranger 1 vs. empty), whereas preference for social novelty was defined by the discrimination index for the novel subject [DI = (stranger 2 exploration time – stranger 1 exploration time)/total exploration time].

Statistical analysis

Data were analysed using the software IBM SPSS Statistics 22.0. We first checked the data for normality (Shapiro-Wilk's test) and homoscedasticity (Levene's test). Next, we evaluated the differences between genotypes by using Student's t-test or Mann-Whitney U test when appropriate. For the resident-intruder test, we also used Chi-square test to compare the number of resident mice displaying aggressive behaviours (attack and chase). Levels of MUPs and *darcin* were qualitative analysed with Image J from the bands obtained in the SDS-PAGE. Briefly, we draw a line through the middle of bands for individual samples and analysed the with and grey value of each band with the Plot Profile command. For social interaction test, we used two-way ANOVA to evaluate the differences with genotype and position as factors. Significance was set at $p < 0.05$.

RESULTS

Distribution of nonapeptidergic cells and fibres is not affected by MeCP2 deficiency

Qualitatively, the distribution of AVP-ir and OT-ir somata and fibres in both *Mecp2*-mutant and WT mice males and females matched with previous reports analysing nonapeptidergic systems in WT mice of two

different strains (Rood et al. 2013; Otero-Garcia et al. 2014). We found abundant AVP-ir cells in the hypothalamic nuclei Pa, SCh, SON, and SOR (Figure 1), and few scattered AVP-ir cells in other areas of the brain such as the AC/ADP, BSTMPI, MeA, and MePD (Figure 2). Similarly, the population of OT-ir cells was abundant in AC/ADP, Pa, SON, and SOR, and sparse in BSTMPI, MeA, and MePD (see examples in Figure 1, 2). Additionally, we observed some co-localization of both neuropeptides in AC/ADP and Pa (not shown), as previously described by Otero-Garcia et al. (2016). In general, we did not find qualitative differences in the distribution of nonapeptidergic somata between males and females.

Regarding AVP-innervation of the telencephalon, we found moderate to dense terminal fields in the LS, vmStP, BST (Figure 3) and Me, and scarce AVP-ir fibres in the ventral hippocampus in WT males, whereas this innervation was reduced in *Mecp2*-null males and both groups of females (see below). In the diencephalon, we found abundant AVP-ir in the periventricular and lateral compartments at preoptic and anterior levels, as well as in the dorsomedial hypothalamic nucleus (DMH) and the lateral habenula (LHb) (Figure 4A), being the latter only significant in WT males (see below). In the mesencephalon, we found AVP-ir in the periaqueductal gray (PAG) and dorsal raphe (DR). As for OT-ir in the telencephalon, we found only a few scattered OT-ir fibres in the nucleus accumbens core (AcbC) and in the shell (AcbSh). Modest OT-ergic innervation was also present in the vmStP, whereas only a few OT-ir terminal fields were present in LS. In the case of BSTMPI, MeA, MePD, central amygdala (Ce) and LHb (Figure 4B) we observed a scarce OT-ergic innervation. Conversely, there was an abundant OT-ergic innervation in the ventrolateral portion of PAG (vlPAG) and DR.

Density of nonapeptidergic cells is not affected by deficits in MeCP2

The analysis of AVP-ir and OT-ir somata revealed that there were no significant differences in cell density between *Mecp2*-het and WT female mice ($p>0.05$ in all cases, Table 2). Likewise, no significant differences were found between *Mecp2*-null and WT males (Figure 5A, B).

Nonapeptidergic innervation is not affected by genotype in *Mecp2*-het females

We did not find significant differences between *Mecp2*-het and WT females in any of the analysed areas, both in AVP-ir and in OT-ir innervation ($p>0.05$ in all cases, Table 3). Thus, the partial deficiency of MeCP2 that occurs in heterozygous individuals fails to affect both the pattern of distribution and the density of nonapeptidergic innervation in young adult female mice.

Testosterone-dependent AVP-ir innervation is reduced in the brain of *Mecp2*-null males

The quantitative analysis of AVP-ir innervation showed significant reduction to absence of AVP-ergic fibres in several sexually dimorphic nuclei in the brain of *Mecp2*-null males (Figure 5C-E). Specifically, AVP-ir innervation was significantly reduced in *Mecp2*-null males in the vmStP (t=3.043, p=0.023), LS (t=2.794, p=0.019), BSTMPI (t=2.569, p=0.028), and LHb (Mann-Whitney, p=0.018). By contrast, immunofluorescent fibres in MeA, MePD and DMH were not significantly different between genotypes (all p>0.05, Figure 5C, D). Additionally, analysis of AVP-ir fibres from DAB immunostaining (Supplementary information, Figure S1) revealed a significant reduction in dorsal endopiriform cortex (dEn) (t=5.009, p=0.002) and ventral hippocampus (vHip) (Mann-Whitney test, p=0.02) of *Mecp2*-null males as compared to WT siblings, but not in dorsolateral PAG (dlPAG), vlPAG or DR (all p>0.05, Figure 6A, B). In the MePD we found a significant effect of genotype in DAB samples (t=2.415, p=0.036) that was not observable in the immunofluorescent samples.

In DAB immunostained samples, we also performed an histochemical detection of NADPH-diaphorase activity, as it helps delimitate the nuclei of interest (Otero-Garcia et al. 2014). Interestingly, NADPH-diaphorase activity has been shown to increase with castration. Given that previous results suggest that the main effect of *Mecp2* genotype was related to a deficit in testosterone-dependent AVP innervation, we checked the density of $NADPHd^{+}$ cells in selected regions of the brain. In agreement with a deficit of testosterone in *Mecp2*-null males, we found a significant increase of $NADPHd^{+}$ cell density in the dorsal and ventral striatum in *Mecp2*-null males as compared to WT, and a general tendency towards increase intensity of labelling in other areas (Supplementary information, Figure S2).

OT-ir innervation is decreased in the lateral habenula of *Mecp2*-null mice

In general, we did not find differences between genotypes in the density of OT-ir innervation (Table 4, all p>0.05) in males, except in the case of the LHb, where we found a significant decrease of OT-ir fibres in *Mecp2*-null males as compared to WT (p=0.02, Figure 4B, B').

Mecp2*-null males do not secrete the male pheromone *darcin

Next we sought to analyse the production of masculine pheromones, dependent on testosterone levels, and specifically of the male pheromone *darcin* (Roberts et al. 2010, 2012). Indeed, female mice do not secrete *darcin* in urine (Supplementary information, Figure S3, Roberts et al. (2010)), and castration, but not some

infections, eliminates the production of *darcin* in WT adult mice (Supplementary information, Figure S3, Lanuza et al. (2014)). Protein electrophoresis of the urine of male mice revealed three to five bands in the urine of WT mice, one corresponding to the 16 kDa MUP *darcin* (Roberts et al. 2010). By contrast, urine samples of *Mecp2*-null males showed only one or two bands, lacking the band corresponding to *darcin* (Figure 7). Moreover, the 20 kDa band, that showed the highest amount of proteins in the urine, was thinner and less intense in *Mecp2*-null mice than in their WT siblings. Thus, *Mecp2*-null males, which have internal testicles, present a pattern of MUPs compatible with low testosterone levels (Roberts et al. 2010; Lanuza et al. 2014).

Mecp2-null males do not attack and display reduced chemoinvestigation of intruders and increased self-grooming

Aggressive behaviour is known to be influenced by testosterone (Brain and Haug 1992). First, we tested WT and *Mecp2*-null mice in a resident-intruder paradigm to evaluate aggressive behaviour against a WT intruder. Since the aggressiveness of our WT males was low, we combined attack and chase parameters and analysed them as one. We found that while 31% of WT resident mice attacked or chased the WT intruder, none of the *Mecp2*-null mice attacked or chased the WT intruder (Chi square test=4.97; p=0.026). However, since the WT resident animals were low aggressive, we did not find significant differences in time spent attacking/chasing the intruder (WT resident: 7.30±2.73 s, *Mecp2*-null resident: 0±0 s, Mann-Whitney U test, p=0.083, Figure 8A).

Additionally, we analysed the time spent by the resident in chemoinvestigation of the intruder, a socially-directed behaviour. Here, *Mecp2*-null male residents spent significantly less time chemoinvestigating the WT intruders, as compared to the time WT residents do towards WT intruders (Mann-Whitney U test, p<0.018) (Figure 8B). All these results point to a lack of interest of *Mecp2*-null males towards their conspecific intruders, at least in the RI-test.

Interestingly, we found that social and agonistic behaviours were apparently substituted in the *Mecp2*-null resident males by self-grooming, as they spent significantly more time grooming than WT residents (Mann-Whitney U test, p=0.005; Figure 8C). Nevertheless, we cannot exclude that this behaviour is reflecting a stereotypic behaviour, similarly to what was reported previously in mouse models of ASD as compared to WT (Chang et al. 2016; Wu et al. 2019).

Since urine analysis has found that *Mecp2*-null males do not secrete the male pheromone *darcin*, we ought to investigate how WT residents would react towards *Mecp2*-null intruders. Thus, we studied aggressive behaviour and chemoinvestigation of an additional group of WT residents presented with *Mecp2*-null intruders, and compared them with the group of WT residents exposed to WT intruders. Data analysis revealed that WT residents investigated significantly more *Mecp2*-null intruders than WT intruders (Student's T-test, $t=-3.882$, $p<0.001$; Figure 8B). By contrast, WT residents did not show significant differences in time spent attacking/chasing WT or *Mecp2*-null intruders (Mann-Whitney U test, $p>0.05$, Figure 8A). This suggests that WT residents "see" *Mecp2*-null animals as "novelty" that calls for their attention/investigation.

Reduced chemoinvestigation of intruders exhibited by *Mecp2*-null males is not due to anosmia

Since both chemoinvestigation and aggressive behaviours are heavily dependent on chemosignals in mice, we checked the olfactory ability of *Mecp2*-null mice in a habituation-dishabituation experiment. In this test, one of the WT animals spent the whole test freezing, whereas one of the *Mecp2*-null males displayed repetitive and aberrant continuous investigation of the cotton swab irrespectively of the presentation, hence both animals were not considered for further analysis. The curves of exploration for each group are depicted in Figure 9A.

First, we checked whether the total time exploring the cotton swab across the whole experiment was affected by genotype. A Student-t test revealed that there was a significant difference between WT and *Mecp2*-null mice in total exploration time ($t=3.863$, $p=0.002$, Figure 9B), with *Mecp2*-null mice displaying a general reduced investigation.

Next, we calculated a discrimination index (DI) as time exploring the first presentation of the odour (rose or urine) minus last presentation of water before each odour. DI for both odours were significantly different from 0 in both genotypes (WT, UrineDI, $t=4.140$, $p=0.009$; RoseDI, $t=3.279$, $p=0.022$; *Mecp2*-null, UrineDI, $t=3.742$, $p=0.005$; RoseDI, $t=2.441$, $p=0.037$), suggesting that both groups of animals were able to discriminate the odours. However, a Student's t test revealed that both UrineDI and RoseDI were significantly different between genotypes ($t=2.639$, $p=0.019$ and $t=3.321$, $p=0.005$, respectively), suggesting that the increase in investigation elicited by both odours was reduced in *Mecp2*-null mice as compared to WT (Figure 9C).

Overall, *Mecp2*-null animals are not anosmic, though they display reduced investigation that could be related to either some degree of hiposmia or, more likely, to the motor demands of the task.

***Mecp2*-null animals show a preference for social contact and social novelty**

Finally, we checked for possible alteration in sociability and social memory by means of social interaction and social recognition tests. In the 3-chamber social interaction test, we first assessed social preference by measuring the time of exploration of each test animal towards a stranger animal (stranger 1) *versus* that of an empty cage. Using a two-way ANOVA we observed a significant *type of stimulus in the cylinder* effect ($F_{1,76}$=103.225, p<0.001), *genotype* effect ($F_{1,76}$=13.039, p=0.001), but also *genotype* x *type of stimulus in the cylinder* interaction effect ($F_{1,76}$= 26.81, p < 0.0001, Figure 10A). Post-hoc comparisons showed that both WT and *Mecp2*-null animals have a social preference, as both spent more time exploring the animal than the empty cage (WTmouse vs. WTempty, t=4,370, p<0.001; *Mecp2*-null_mouse vs. *Mecp2*-null_empty, t=9,334, p<0.001). Interestingly, *Mecp2*-null spent significantly more time than WT animals exploring the stranger mouse 1 (t = 6,214, p<0.001).

Next, a novel animal (stranger 2) was placed in the previously empty cylinder and social recognition was evaluated. A statistically significant main effect of *genotype* ($F_{1,76}$= 12.614, p=0.001; Figure 10B) was observed. Overall, both WT and *Mecp2*-null animals recognized stranger 2 as novelty since they spent more time investigating stranger 2 than stranger 1 (main effect of *position*; $F_{1,76}$=11.205, p<0.001). Moreover, *Mecp2*-null animals explore for significantly more time strangers 1 and 2 than WT animals. Overall, data from these experiments suggest that *Mecp2*-null animals seek social contact when tested in a new environment.

DISCUSSION

In this study, we investigated the distribution and density of nonapeptidergic somata and innervation in young adult *Mecp2*-null males and *Mecp2*-het females, as compared to their WT siblings. Overall, females do not show significant differences between genotypes in either AVP-ergic or OT-ergic distribution. By contrast, we found a significant reduction in AVP innervation in *Mecp2*-null males, specifically in the sexually dimorphic nuclei of the social brain network. Additionally, we found in *Mecp2*-null males a significant reduction of OT innervation specifically in the LHb, which is not sexually dimorphic.

Since the main neuroanatomical changes found in the nonapeptidergic system were specific to the testosterone-dependent AVP-ergic innervation, we further analysed features that are dependent on the gonadal status of males. Specifically, we analysed the production of urinary pheromones as a proxy of testosterone level and aggressive and social behaviours, and found significant deficits in all of them that we discuss below.

The distribution of AVP and OT cells is not affected by lack or deficit of MeCP2

AVP and OT are both synthesised in the Pa and SON hypothalamic nuclei. Besides, AVP-ir somata are also present in the SCh and AVP-ir and scarce OT-ir somata in Me, BST and accessory nuclei. Distribution of AVP and OT in our sample of WT and *Mecp2*-mutant mice matched previous studies in mice by Otero-Garcia et al., (2014; 2016) in CD1 strain and Rood et al (2013) in C57BL/6N strain. In general, neurons were either AVP-ir or OT-ir, although we found co-localization of both neuropeptides in AC/ADP and Pa, as previously described (Otero-Garcia et al. 2016).

These results suggest that deletion of MeCP2, previously described as key in the regulation of AVP in the Pa (Murgatroyd et al. 2009), is not sufficient to produce a major deficit in AVP production. To our knowledge, a regulation of the OT gene by MeCP2 has not been described, however, the AVP and OT genes are located in adjacent regions of the same chromosome, separated only by 12 Kb (Summar et al. 1990), and both peptides are co-expressed in some neuronal populations (Otero-Garcia et al., 2016), suggesting a close transcriptional regulation of both genes. As with AVP, no qualitative differences were observed in OT distribution between genotypes. However, a caveat in this study is that immunohistochemistry is not directly quantitative of the level of nonapeptides. Thus, future experiments should address the possibility that nonapeptidergic mRNA or protein levels are affected in *Mecp2*-mutant mice.

***Mecp2*-heterozygous females show no deficits in the nonapeptidergic systems**

We did not find significant differences in nonapeptidergic distribution or innervation between *Mecp2*-het females and their WT littermates. Lack of differences between genotypes in females could be attributed to i) the presence of one *Mecp2* allele in females that could be sufficient to prevent alterations in AVP or to ii) a lack of testosterone-dependent AVP innervation in females, assuming that absence of AVP in sexually dimorphic nuclei in *Mecp2*-null males is mainly testosterone-dependent. In addition, we must also consider possible age-effects in our mice, analysed at 8 weeks old. At this age, male *Mecp2*-null mice are already

manifesting the overt phenotype of the syndrome, whereas female *Mecp2*-het mice do not show the complete symptomatology until, at least, 3 months old (Guy et al. 2001). In this sense, further investigations of AVP/OT-ergic systems in older females are required to elucidate possible impairments in both nonapeptidergic systems.

Mecp2-null males exhibit significant deficits in testosterone-dependent AVP-ergic innervation and OT-ir in LHb

As described in previous reports (Rood et al. 2013; Otero-Garcia et al. 2014), AVP-ergic innervation is sexually dimorphic in some brain nuclei. Specifically, Rood et al., (2013) described that AVP-ergic innervation of LS, Me, BST, LHb, PAG, vHip, and DR nuclei was dependent on gonadal steroids and more abundant in males than in females, whereas AVP fibres in hypothalamic areas such as DMH were not dependent on gonadal steroids and did not show sex differences. Our data in *Mecp2*-null mice show that there is a specific decrease in AVP-ergic innervation in all the testosterone-dependent nuclei, but not in the DMH. Thus, our data is consistent with an effect of lack MeCP2 in AVP production through indirect testosterone-dependent mechanisms. In this sense, Auger and collaborators (2011) showed that circulating gonadal steroid hormones modify the methylation status of some steroid responsive gene promoters and, consequently their expression levels. In accordance, methylation of *AVP* promoter is regulated by testosterone signalling in the BST of adult male rats (Auger et al. 2011). Moreover, sexually-dimorphic AVP-ir innervation in the LS is dependent on the action of estradiol (presumably aromatised from testosterone) via ERα receptor (Scordalakes and Rissman 2004), which is also regulated by MeCP2 in the brain (Westberry et al. 2010). *Mecp2*-null males display internal testicles (Guy et al. 2001), a feature consistent with lower levels of testosterone production and possible deficits in signalling through ERα (Cederroth et al. 2007). Although future studies ought to directly measure androgen levels in *Mecp2*-null mice to prove a reduction in testosterone levels, our data showing that *Mecp2*-null males display a reduction of MUPs and lack the masculine pheromone *darcin* support this assumption. We acknowledge that other deficits displayed by *Mecp2*-null males, such as specific deficits in pheromonal production or impaired kidney function, could account for this physiological effect, but we think that the most likely explanation is that of reduced testosterone levels. Indeed, *darcin* production is absent in females and castrated males but present in "sick" males (see Supplementary information).

In addition to an indirect action through hormonal deficits, deficits in MeCP2 have been shown to directly regulate the sexually-dimorphic AVP-ir innervation in rats. Thus, a transient reduction of MeCP2 during the first three post-natal days via focal injections of siRNA in the Me, lead to a transient decrease of both androgen receptor (AR) and AVP mRNA in the Me of 14 days old rat males (Forbes-Lorman et al. 2012). Interestingly, rats subjected to this treatment at early postnatal days showed no lasting effects on the levels of AR at 7.5 months old, but a long-lasting deficit in the density of AVP-ir somata in centromedial amygdala and BST, and a reduction of LS innervation. In fact, the expression of *Mecp2* gene is sexually dimorphic in the brain of rats during the steroid-sensitive period (Kurian et al. 2007), suggesting a key role of this gene in the development of sexually-dimorphic systems. In summary, the mechanism by which MeCP2 regulates AVP production may be an indirect effect over gonadal hormone production, a direct gene regulation, or both.

Surprisingly, we also found a significant decrease in the scarce OT innervation in LHb, a feature that, to our knowledge, has not been previously described as sexually dimorphic, in our *Mecp2*-null males compared to their WT siblings. Low levels of testosterone could also contribute to this deficit, since the metabolite of dihydrotestosterone, 5α-androstane-3β,17β-diol, is able to regulate OT expression through ER-β activation (Hiroi et al. 2013), a type of estrogenic receptor found in the LHb (Shughrue et al. 1997).

Consequences of nonapeptidergic deficits for behaviour in *Mecp2*-null mice

Alterations in AVP-ergic and OT-ergic signalling may impair the proper functioning of the social brain network. For instance, deficits in AVP-ergic innervation in BST/Me and nuclei to which they project, could be affecting social and aggressive behaviours in *Mecp2*-null males (Modi and Sahin 2018), which is consistent with our results obtained in the RI test (see below). The MePD is interconnected with BSTPM to control socio-sexual behaviours mediated by pheromones, as well as defensive behaviours against predators (Pardo-Bellver et al. 2012; Tong et al. 2019). Both MePD and BST are intimately modulated by circulating hormones such as progestogens, androgens and oestrogens (De Lorme et al. 2012; Pardo-Bellver et al. 2012; Zancan et al. 2017) due to the large number of cells that express steroid receptors. Despite the extensive innervation of AVP in MePD, the density of V1aR is sparse, and how the AVP could modulate social behaviour in adult males remains poorly understood (Smith et al. 2019). Finally, LS and vHip are connected to each other, allowing LS to integrate socio-sexual information from the amygdala with spatial and contextual information from the vHip (Campbell et al. 2009; Pardo-Bellver et al. 2012). This pathway

provides adequate responses to each social situation and, therefore, it has been proposed that its connectivity could be impaired in ASD patients.

It was recently found that LHb is involved in the regulation of social preference in rats (Benekareddy et al. 2018) and aggression in mice (Golden et al. 2016). Therefore, deficits of both AVP- and OT-ergic innervation in this structure could contribute to the social abnormalities displayed by *Mecp2*-null mice. LHb integrates information from the hypothalamus. In this sense, the LHb regulates the serotoninergic system between the DR and other nuclei such as the amygdala, BST, LS, hippocampus, and preoptic area (Rood et al. 2013). Serotonin, together with NO and AVP, modulate social and aggressive behaviours in rodents (Ferris et al. 1997; Agustín-Pavón et al. 2009; Angoa-Pérez and Kuhn 2015; Hashikawa et al. 2017). Whereas serotonin blocks aggression and territorial behaviour, AVP in the anterior hypothalamus promotes aggression in males. It has been described that serotonin agonists promote AVP and OT synthesis. Likewise, AVP administration stimulates synthesis and release of serotonin in some brain nuclei (Auerbach and Lipton 1982; Jørgensen et al. 2003). In support of this hypothesis, deficit in serotonin levels has previously been reported in *Mecp2*-null males (Santos et al. 2010; Vogelgesang et al. 2017). Likewise, treatments based on stimulation of the serotonin transmission are able to improve the phenotype of *Mecp2*-null males (Ricceri et al. 2013) and *Mecp2*-het females (Filippis et al. 2015). Consequently, it is likely that lack of MeCP2, causing misbalances in the metabolism of NO and serotonin and production of gonadal hormones, could be affecting AVP- and OT-ergic innervation in a region-specific manner and, therefore, impairing social and aggressive behaviours in *Mecp2*-null mice.

Abnormal aggression and social behaviour in *Mecp2*-null males

In the RI test, *Mecp2*-null residents do not display aggressive behaviours against the intruder, which is consistent with a decreased AVP innervation and increased $NADPHd^{+}$ (indicative of increased production of NO) found in those males. Both, AVP and NO have been long related with the modulation of aggressive behaviours in male mice (Trainor et al. 2007; Robinson et al. 2012; Marie-Luce et al. 2013). Thus, decreased AVP innervation (in particular in the LS, Veenema et al., (2010)), and possibly an increase in NO production in the brain of our *Mecp2*-null males, could contribute to the alterations found in *Mecp2*-null behaviours in the RI test, such as reduced aggression of the intruder and territoriality. Interestingly, it has been shown that overexpression of MeCP2 can increase aggressive behaviour both in mice and humans (Tantra et al. 2014), in agreement with the lack of aggression that we found in *Mecp2*-null mice.

Of note, we cannot exclude the possibility that, being *Mecp2*-null mice smaller than the WT intruders, this can constitute a confounding factor in the results obtained, as the size of WT animals can be "intimidatory" towards the smaller *Mecp2*-null animals. In addition, we found a reduction in chemoinvestigation of the intruder by *Mecp2*-null males, which is not explained by anosmia, as results from the habituation-dishabituation test showed that both WT and *Mecp2*-null males are able to detect both urine and rose odours. Instead, the reduced chemoinvestigation points towards a general lack of interest in the intruder by *Mecp2*-null residents. Another possibility is that *Mecp2*-null animals exhibit behaviours such as self-grooming, an activity to which they devoted about a 13% of the time of the test, whereas WT residents devoted a mere 1.6% of the time to this behaviour. Finally, we did not directly measure locomotion in these tasks, so potential locomotor deficits of *Mecp2*-null mice could influence the observed results.

Curiously, *Mecp2*-null intruders were significantly more investigated by WT residents. Provided that male sexual pheromones give information about strain, sex and fertility of rodents (Brennan and Kendrick 2006), and that *Mecp2*-null males show low levels of MUPs and *darcin* in the urine, we suggest that increased investigation of *Mecp2*-null intruders by WT residents could be due to lack of information given by male pheromones. In this line it would be interesting in future studies to further explore the social dimension of *Mecp2*-null mice in social interaction tests, including the use of *Mecp2*-null mice as stimulus animals and exploring the behavioural features of and towards *Mecp2*-het females.

The apparent lack of interest in the conspecific intruder displayed by *Mecp2*-null males in the RI test is in sharp contrast with the results of the social interaction/recognition test, where *Mecp2*-null males not only displayed a stronger social preference behaviour than their WT siblings, but also a significant social recognition. Regarding a possible increase in seeking social contact in our *Mecp2*-null males, this result was previously obtained with other models of RTT. Thus, *Mecp2*^{1lox} (Chen et al. 2001) and Mecp2$^{308/y}$ show increased social preference as compared to WT (Schaevitz et al. 2010; Pobbe et al. 2012). In agreement, whilst overexpression of *Mecp2* promotes autistic-like behaviours in *Mecp2* mutant mice (Peters et al. 2013) and in *MECP2* transgenic monkeys (Liu et al. 2016), the genetic deletion of *Mecp2* in rodents might increase social preference. In this sense, even though traditionally RTT has been grouped under the umbrella of ASD, the recent revision of the Diagnostic and Statistical Manual of Mental Disorders (DSM) removed RTT from the ASD category (Lai et al. 2013).

The increased social recognition that *Mecp2*-null males show is consistent with previous results from Schaevitz et al., (2010), and suggest that lack of MeCP2 does not impair social recognition. In this regard, previous reports attributed to oxytocinergic signalling a role in the modulation of social recognition memory in the rodent brain (Gur et al. 2014; Zalla 2014). In this line, the lack of differences we found in our experiments in the OT-ergic distribution and innervation in most of the social brain of our *Mecp2*-null males might support why social recognition is not impaired in these mice. Additionally, explorative behaviour in this second test was again significantly higher in *Mecp2*-null males compared to WT, reinforcing the hypothesis of elevated seeking of social contact in those males. This result could also be related to differences in anxiety when tested in a novel environment, which is reduced in *Mecp2*-null mice (Stearns et al., 2007) (and our own observations). However, it should be noted that our results on social behaviour and those by Schaevitz et al., (2010) contrast with several studies. For example, in a recent report, Phillips et al., (2019) found that *Mecp2* KO displayed acute deficits in social memory, that could be rescued upon inactivation of a hyperactive vHip-PFC circuit in these mice. However, one can find several differences between this study and ours, among which are both the mouse model and the age of the animals (younger in the study by Phillips et al. (2019)).

Conclusions and future directions

Taken together, our results in *Mecp2*-null male mice reveal several abnormalities in sexually-dimorphic, testosterone-dependent, neuroanatomical (nonapeptidergic innervation), physiological (pheromone production) and behavioural features (aggression and sociality). These deficits could be due both to a direct involvement of MeCP2 in the regulation of expression of several genes (AVP, ERα) or to indirect effects due to the impact of lack MeCP2 in gonadal development, and consequently in the hormonal status of the mice. Thus, when studying neurodevelopmental disorders such as RTT and other MECP2 related conditions, it is important to consider possible effects in hormonal signalling that could account for some of the deficits observed. In this sense, differences in levels of gonadal hormones have been implicated in sexual differences in the incidence and severity of some diseases such as autism, and psychiatric and cognitive disorders (Romano et al. 2016; Akinola and Gabriel 2018). Future studies should study in depth the mechanism leading to the loss of sexually-dimorphic features in *Mecp2*-null males, and check the possible effect of pharmacological manipulations of nonapeptidergic systems in the amelioration of behavioural symptoms in this mouse model.

REFERENCES

Agustín-Pavón C, Martínez-Ricós J, Martínez-García F, Lanuza E (2009) Role of nitric oxide in pheromone-mediated intraspecific communication in mice. Physiol Behav 98:608–613.

Akinola OB, Gabriel MO (2018) Neuroanatomical and molecular correlates of cognitive and behavioural outcomes in hypogonadal males. Metab Brain Dis 33:491–505. doi: 10.1007/s11011-017-0163-5

Angoa-Pérez M, Kuhn DM (2015) Neuronal serotonin in the regulation of maternal behavior in rodents.

Auerbach S, Lipton P (1982) Vasopressin augments depolarization-induced release and synthesis of serotonin in hippocampal slices. J Neurosci 2:477–82.

Auger CJ, Coss D, Auger AP, Forbes-Lorman RM (2011) Epigenetic control of vasopressin expression is maintained by steroid hormones in the adult male rat brain. Proc Natl Acad Sci 108:4242–4247. doi: 10.1073/pnas.1100314108

Benekareddy M, Stachniak TJ, Bruns A, et al (2018) Identification of a Corticohabenular Circuit Regulating Socially Directed Behavior. Biol Psychiatry. doi: 10.1016/j.biopsych.2017.10.032

Brain PB, Haug M (1992) Hormonal and neurochemical correlates of various forms of animal "aggression." Psychoneuroendocrinology

Brennan P a, Kendrick KM (2006) Mammalian social odours: attraction and individual recognition. Philos Trans R Soc Lond B Biol Sci 361:2061–78. doi: 10.1098/rstb.2006.1931

Campbell P, Ophir AG, Phelps SM (2009) Central vasopressin and oxytocin receptor distributions in two species of singing mice. J Comp Neurol 516:321–333. doi: 10.1002/cne.22116

Cederroth CR, Schaad O, Descombes P, et al (2007) Estrogen receptor α is a major contributor to estrogen-mediated fetal testis dysgenesis and cryptorchidism. Endocrinology. doi: 10.1210/en.2007-0689

Chang AD, Berges VA, Chung SJ, et al (2016) High-Frequency Stimulation at the Subthalamic Nucleus Suppresses Excessive Self-Grooming in Autism-Like Mouse Models. Neuropsychopharmacology 41:1813–1821. doi: 10.1038/npp.2015.350

Chen RZ, Akbarian S, Tudor M, Jaenisch R (2001) Deficiency of methyl-CpG binding protein-2 in CNS

neurons results in a Rett-like phenotype in mice. Nat Genet. doi: 10.1038/85906

Christodoulou CEJ (2001) Rett syndrome: clinical characteristics and recent genetic advances. Disabil Rehabil 23:98–106. doi: 10.1080/09638280150504171

De Lorme KC, Schulz KM, Salas-Ramirez KY, Sisk CL (2012) Pubertal testosterone organizes regional volume and neuronal number within the medial amygdala of adult male Syrian hamsters. Brain Res 1460:33–40. doi: 10.1016/j.brainres.2012.04.035

Domes G, Heinrichs M, Michel A, et al (2007) Oxytocin Improves “Mind-Reading” in Humans. Biol Psychiatry 61:731–733. doi: 10.1016/j.biopsych.2006.07.015

Ferris CF, Melloni RH, Koppel G, et al (1997) Vasopressin/serotonin interactions in the anterior hypothalamus control aggressive behavior in golden hamsters. J Neurosci 17:4331–40. doi: 10.1523/JNEUROSCI.17-11-04331.1997

Filippis B De, Chiodi V, Adriani W, et al (2015) Long-lasting beneficial effects of central serotonin receptor 7 stimulation in female mice modeling Rett syndrome. Front Behav Neurosci 9:86. doi: 10.3389/FNBEH.2015.00086

Forbes-Lorman RM, Rautio JJ, Kurian JR, et al (2012) Neonatal MeCP2 is important for the organization of sex differences in vasopressin expression. Epigenetics 7:230–238. doi: 10.4161/epi.7.3.19265

Francis SM, Sagar A, Levin-Decanini T, et al (2014) Oxytocin and vasopressin systems in genetic syndromes and neurodevelopmental disorders. Brain Res 1580:199–218. doi: 10.1016/j.brainres.2014.01.021

Freeman SM, Palumbo MC, Lawrence RH, et al (2018) Effect of age and autism spectrum disorder on oxytocin receptor density in the human basal forebrain and midbrain. Transl Psychiatry 8:257. doi: 10.1038/s41398-018-0315-3

Golden SA, Heshmati M, Flanigan M, et al (2016) Basal forebrain projections to the lateral habenula modulate aggression reward. Nature. doi: 10.1038/nature18601

Goodson J (2008) Nonapeptides and the evolutionary patterning of sociality. In: Advances in Vasopressin and Oxytocin — From Genes to Behaviour to Disease. Elsevier, pp 3–15

Gur R, Tendler A, Wagner S (2014) Long-Term Social Recognition Memory Is Mediated by Oxytocin-

Dependent Synaptic Plasticity in the Medial Amygdala. Biol Psychiatry 76:377–386. doi: 10.1016/j.biopsych.2014.03.022

Guy J, Hendrich B, Holmes M, et al (2001) A mouse Mecp2-null mutation causes neurological symptoms that mimic rett syndrome. Nat Genet 27:322–326. doi: 10.1038/85899

Hagberg B (2002) Clinical manifestations and stages of Rett syndrome. Ment Retard Dev Disabil Res Rev 8:61–65. doi: 10.1002/mrdd.10020

Hashikawa Y, Hashikawa K, Falkner AL, Lin D (2017) Ventromedial Hypothalamus and the Generation of Aggression. Front Syst Neurosci 11:1–13. doi: 10.3389/fnsys.2017.00094

Hiroi R, Lacagnina AF, Hinds LR, et al (2013) The androgen metabolite, 5α-androstane-3β,17β-diol (3β-diol), activates the oxytocin promoter through an estrogen receptor-β pathway. Endocrinology 154:1802–12. doi: 10.1210/en.2012-2253

Jørgensen H, Riis M, Knigge U, et al (2003) Serotonin Receptors Involved in Vasopressin and Oxytocin Secretion. J Neuroendocrinol 15:242–249. doi: 10.1046/j.1365-2826.2003.00978.x

Kurian JR, Forbes-Lorman RM, Auger AP (2007) Sex difference in Mecp2 expression during a critical period of rat brain development. Epigenetics. doi: 10.4161/epi.2.3.4841

Lai M-C, Lombardo M V., Chakrabarti B, Baron-Cohen S (2013) Subgrouping the Autism "Spectrum": Reflections on DSM-5. PLoS Biol 11:e1001544. doi: 10.1371/journal.pbio.1001544

Lanuza E, Martín-Sánchez A, Marco-Manclús P, et al (2014) Sex pheromones are not always attractive: changes induced by learning and illness in mice. Anim Behav 97:265–272. doi: 10.1016/J.ANBEHAV.2014.08.011

LaSalle JM, Goldstine J, Balmer D, Greco CM (2001) Quantitative localization of heterogeneous methyl-CpG-binding protein 2 (MeCP2) expression phenotypes in normal and Rett syndrome brain by laser scanning cytometry. Hum Mol Genet 10:1729–40.

Liu Z, Li X, Zhang J-T, et al (2016) Autism-like behaviours and germline transmission in transgenic monkeys overexpressing MeCP2. Nature 530:98–102. doi: 10.1038/nature16533

Lukas M, Neumann ID (2013) Oxytocin and vasopressin in rodent behaviors related to social dysfunctions in autism spectrum disorders. Behav Brain Res 251:85–94. doi:

10.1016/j.bbr.2012.08.011

Marie-Luce C, Raskin K, Bolborea M, et al (2013) Effects of neural androgen receptor disruption on aggressive behavior, arginine vasopressin and galanin systems in the bed nucleus of stria terminalis and lateral septum. Gen Comp Endocrinol 188:218–225. doi: 10.1016/j.ygcen.2013.03.031

Martínez-Rodríguez E, Martín-Sánchez A, Coviello S, et al (2019) Lack of MeCP2 leads to region-specific increase of doublecortin in the olfactory system. Brain Struct Funct. doi: 10.1007/s00429-019-01860-6

Menon R, Grund T, Zoicas I, et al (2018) Oxytocin Signaling in the Lateral Septum Prevents Social Fear during Lactation. Curr Biol 28:1066-1078.e6. doi: 10.1016/j.cub.2018.02.044

Miller M, Bales KL, Taylor SL, et al (2013) Oxytocin and Vasopressin in Children and Adolescents With Autism Spectrum Disorders: Sex Differences and Associations With Symptoms. Autism Res 6:91–102. doi: 10.1002/aur.1270

Modahl C, Green L, Fein D, et al (1998) Plasma oxytocin levels in autistic children. Biol Psychiatry 43:270–7.

Modi ME, Sahin M (2018) A unified circuit for social behavior. Neurobiol Learn Mem. doi: 10.1016/j.nlm.2018.08.010

Murgatroyd C, Patchev A V., Wu Y, et al (2009) Dynamic DNA methylation programs persistent adverse effects of early-life stress. Nat Neurosci 12:1559–1566. doi: 10.1038/nn.2436

Newman SW (1999) The medial extended amygdala in male reproductive behavior. A node in the mammalian social behavior network. In: Annals of the New York Academy of Sciences. pp 242–257

Otero-Garcia M, Agustín-Pavón C, Lanuza E, Martínez-García F (2016) Distribution of oxytocin and co-localization with arginine vasopressin in the brain of mice.

Otero-García M, Agustín-Pavón C, Lanuza E, Martínez-García F (2015) Distribution of oxytocin and co-localization with arginine vasopressin in the brain of mice. Brain Struct Funct 221:3445–3473. doi: 10.1007/s00429-015-1111-y

Otero-Garcia M, Martin-Sanchez A, Fortes-Marco L, et al (2014) Extending the socio-sexual brain:

Arginine-vasopressin immunoreactive circuits in the telencephalon of mice. Brain Struct Funct 219:1055–1081.

Pardo-Bellver C, Cádiz-Moretti B, Novejarque A, et al (2012) Differential efferent projections of the anterior, posteroventral, and posterodorsal subdivisions of the medial amygdala in mice. Front Neuroanat 6:1–26. doi: 10.3389/fnana.2012.00033

Paxinos G, Franklin K (2012) Paxinos and Franklin's the Mouse Brain in Stereotaxic Coordinates. In: Acad. Press. https://www.elsevier.com/books/paxinos-and-franklins-the-mouse-brain-in-stereotaxic-coordinates/paxinos/978-0-12-391057-8.

Peters SU, Hundley RJ, Wilson AK, et al (2013) The Behavioral Phenotype in *MECP 2* Duplication Syndrome: A Comparison With Idiopathic Autism. Autism Res 6:42–50. doi: 10.1002/aur.1262

Phillips ML, Robinson HA, Pozzo-Miller L (2019) Ventral hippocampal projections to the medial prefrontal cortex regulate social memory. Elife. doi: 10.7554/eLife.44182

Pobbe RLH, Pearson BL, Blanchard DC, Blanchard RJ (2012) Oxytocin receptor and Mecp2 308/Y knockout mice exhibit altered expression of autism-related social behaviors. Physiol Behav 107:641–8. doi: 10.1016/j.physbeh.2012.02.024

Ramocki MB, Tavyev YJ, Peters SU (2010) The *MECP2* duplication syndrome. Am J Med Genet Part A. doi: 10.1002/ajmg.a.33184

Rett A (2016) On a remarkable syndrome of cerebral atrophy associated with hyperammonaemia in childhood. Wiener Medizinische Wochenschrift 166:322–324. doi: 10.1007/s10354-016-0492-8

Rett A (1966) [On a unusual brain atrophy syndrome in hyperammonemia in childhood]. Wien Med Wochenschr 116:723–6.

Ricceri L, De Filippis B, Laviola G (2013) Rett syndrome treatment in mouse models: Searching for effective targets and strategies. Neuropharmacology 68:106–115.

Roberts S a., Davidson AJ, McLean L, et al (2012) Pheromonal induction of spatial learning in mice. Science (80-) 338:1462–5. doi: 10.1126/science.1225638

Roberts SA, Simpson DM, Armstrong SD, et al (2010) Darcin: a male pheromone that stimulates female memory and sexual attraction to an individual male's odour. BMC Biol 8:75. doi: 10.1186/1741-

7007-8-75

Robinson S, Penatti CAA, Clark AS (2012) The role of the androgen receptor in anabolic androgenic steroid-induced aggressive behavior in C57BL/6J and Tfm mice. Horm Behav 61:67–75. doi: 10.1016/j.yhbeh.2011.10.004

Romano E, Cosentino L, Laviola G, De Filippis B (2016) Genes and sex hormones interaction in neurodevelopmental disorders. Neurosci Biobehav Rev 67:9–24. doi: 10.1016/j.neubiorev.2016.02.019

Rood BD, Stott RT, You S, et al (2013) Site of origin of and sex differences in the vasopressin innervation of the mouse (Mus musculus) brain. J Comp Neurol. doi: 10.1002/cne.23288

Santos M, Summavielle T, Teixeira-Castro A, et al (2010) Monoamine deficits in the brain of methyl-CpG binding protein 2 null mice suggest the involvement of the cerebral cortex in early stages of Rett syndrome. Neuroscience. doi: 10.1016/j.neuroscience.2010.07.010

Santos M, Temudo T, Kay T, et al (2009) Mutations in the MECP2 gene are not a major cause of rett syndrome-like or related neurodevelopmental phenotype in male patients. J Child Neurol. doi: 10.1177/0883073808321043

Schaevitz LR, Moriuchi JM, Nag N, et al (2010) Cognitive and social functions and growth factors in a mouse model of Rett syndrome. Physiol Behav 100:255–263. doi: 10.1016/j.physbeh.2009.12.025

Scordalakes EM, Rissman EF (2004) Aggression and arginine vasopressin immunoreactivity regulation by androgen receptor and estrogen receptor α. Genes, Brain Behav. doi: 10.1111/j.1601-183X.2004.00036.x

Shughrue PJ, Lane M V., Merchenthaler I (1997) Comparative distribution of estrogen receptor-α and -β mRNA in the rat central nervous system. J Comp Neurol. doi: 10.1002/(SICI)1096-9861(19971201)388:4<507::AID-CNE1>3.0.CO;2-6

Smith CJW, DiBenedictis BT, Veenema AH (2019) Comparing vasopressin and oxytocin fiber and receptor density patterns in the social behavior neural network: Implications for cross-system signaling. Front Neuroendocrinol 53:100737. doi: 10.1016/j.yfrne.2019.02.001

Stearns NA, Schaevitz LR, Bowling H, et al (2007) Behavioral and anatomical abnormalities in Mecp2

mutant mice: A model for Rett syndrome. Neuroscience. doi: 10.1016/j.neuroscience.2007.02.009

Summar ML, Phillips J a, Battey J, et al (1990) Linkage relationships of human arginine vasopressin-neurophysin-II and oxytocin-neurophysin-I to prodynorphin and other loci on chromosome 20. Mol Endocrinol 4:947–50. doi: 10.1210/mend-4-6-947

Tantra M, Hammer C, Kästner A, et al (2014) Mild expression differences of MECP2 influencing aggressive social behavior. EMBO Mol Med. doi: 10.1002/emmm.201303744

Tong WH, Abdulai-Saiku S, Vyas A (2019) Testosterone Reduces Fear and Causes Drastic Hypomethylation of Arginine Vasopressin Promoter in Medial Extended Amygdala of Male Mice. Front Behav Neurosci 13:33. doi: 10.3389/fnbeh.2019.00033

Trainor BC, Workman JL, Jessen R, Nelson RJ (2007) Impaired Nitric Oxide Synthase Signaling Dissociates Social Investigation and Aggression. Behav Neurosci. doi: 10.1037/0735-7044.121.2.362

Veenema AH, Beiderbeck DI, Lukas M, Neumann ID (2010) Distinct correlations of vasopressin release within the lateral septum and the bed nucleus of the stria terminalis with the display of intermale aggression. Horm Behav. doi: 10.1016/j.yhbeh.2010.03.006

Vogelgesang S, Niebert S, Renner U, et al (2017) Analysis of the Serotonergic System in a Mouse Model of Rett Syndrome Reveals Unusual Upregulation of Serotonin Receptor 5b. Front Mol Neurosci 10:61. doi: 10.3389/fnmol.2017.00061

Waterhouse L, Fein D, Modahl C (1996) Neurofunctional mechanisms in autism. Psychol Rev 103:457–89.

Westberry JM, Trout AL, Wilson ME (2010) Epigenetic regulation of estrogen receptor α gene expression in the mouse cortex during early postnatal development. Endocrinology. doi: 10.1210/en.2009-0955

Winslow JT, Insel TR (2004) Neuroendocrine basis of social recognition. Curr Opin Neurobiol 14:248–253. doi: 10.1016/j.conb.2004.03.009

Wu W-L, Cheng S-J, Lin S-H, et al (2019) The Effect of ASIC3 Knockout on Corticostriatal Circuit and Mouse Self-grooming Behavior. Front Cell Neurosci 13:86. doi: 10.3389/fncel.2019.00086

Zalla T (2014) Amygdala, Oxytocin, and Social Cognition in Autism Spectrum Disorders. Biol Psychiatry 76:356–357. doi: 10.1016/J.BIOPSYCH.2014.06.022

Zancan M, Dall'Oglio A, Quagliotto E, Rasia-Filho AA (2017) Castration alters the number and structure of dendritic spines in the male posterodorsal medial amygdala. Eur J Neurosci 45:572–580. doi: 10.1111/ejn.13460

Zoghbi HY, Amir RE, Van den Veyver IB, et al (1999) Rett syndrome is caused by mutations in X-linked MECP2, encoding methyl-CpG-binding protein 2. Nat Genet 23:185–188. doi: 10.1038/13810

FIGURE LEGENDS

Figure 1. Representative pictures of AVP- (green) and OT-ergic (red) somata in four hypothalamic regions of WT and *Mecp2*-null males. AVP and OT-ir somata in hypothalamic A, A') paraventricular, B) suprachiasmatic, C) supraoptic and D, D') the retroquiasmatic part of the supraoptic nucleus. The distribution and density of AVP and OT-ir somata in *Mecp2*-null or *Mecp2*-het mice do not differ from WT mice. Scale bar 100µm. Abbreviations: 3V: 3rd ventricle; Pa: paraventricular hypothalamic nucleus; Pe: periventricular hypothalamic nucleus; SCh: suprachiasmatic nucleus; SON: supraoptic nucleus; SOR: retroquiasmatic part of the supraoptic nucleus

Figure 2. Representative pictures of AVP- (green) and OT-ergic (red) immunofluorescence in three brain regions of WT and *Mecp2*-null males. AVP and OT-ir in A, A') nucleus of the anterior commissure / anterodorsal preoptic nucleus region, B, B') bed nucleus of the stria terminalis, medial division, and C, C') medial amygdala. The distribution and density of AVP and OT-ir somata in *Mecp2*-null or *Mecp2*-het mice do not differ from WT mice. Scale bar 100µm. Abbreviations: 3V: 3rd ventricle; AC/ADP: nucleus of the anterior commissure / anterodorsal preoptic nucleus region; BSTMPI: bed nucleus of the stria terminalis, medial division; Me: medial amygdala; Opt: optic tract; Pe: periventricular hypothalamic nucleus.

Figure 3. Representative pictures of AVP-immunofluorescence (green) and DAPI labelling (blue) in three brain regions of WT and *Mecp2*-null males. Arrows point to AVP-ir fibres. Testosterone-dependent AVP-ergic innervation in the lateral septum (A, A'), ventromedial striato-pallidum (B, B') and bed nucleus of the stria terminalis (C, C') was significantly reduced in *Mecp2*-null males as compared to WT males. Scale bar 100µm. Abbreviations: BSTMPI: bed nucleus of the stria terminalis, medial division; LS: lateral septum; vmStP: .ventromedial striatopallidum.

Figure 4. Representative pictures of AVP- (green) and OT-ergic (red) immunofluorescence and DAPI labelling (blue) in the lateral habenula of WT and *Mecp2*-null males. Arrows point to immunofluorescent APV-ergic and OT-ergic fibres. Both AVP (A, A') and OT-ir (B, B') innervation was significantly reduced in *Mecp2*-null as compared to WT mice. Scale bar 100µm. Abbreviations: LHb: lateral habenular nucleus, MHb: medial habenular nucleus.

Figure 5. Bar chart showing the density of AVP-immunofluorescent (cells/mm^2) (A, B) and fibres crossings (C, D) in different brain nuclei of WT (black bars) and *Mecp2*-null males (white bars). Due to the intricate

mark of AVP found in the LHab, we represent the number of squares instead of crosses of fibres for this nucleus (E). Statistical analyses (Student's T-test or Mann-Whitney U test) revealed no effect of genotype for AVP-ir cell density (A, B), but a significant reduction of testosterone-dependent AVP-ergic innervation in *Mecp2*-null males as compared WT siblings (C-E). Values are presented as mean ± SEM. *=p<0.05

Figure 6. Bar chart showing AVP-ir innervation in samples immunostained with DAB, in WT (black bars) and *Mecp2*-null males (white bars). Similar to AVP-ir assayed by immunofluorescence, results from statistical analyses (Student's T-test or Mann-Whitney U test) showed a significant decrease of testosterone-dependent AVP-ergic innervation in *Mecp2*-null males as compared to WT. Values are presented as mean ± SEM. *=p<0.05; **=p<0.01

Figure 7. A. Protein electrophoresis of the urine of WT and *Mecp2*-null males. Approximately 50 µg of total protein were loaded (except in the WT male marked with *, for which we did not have enough sample). The band corresponding to *darcin* can be clearly appreciated in three of the four WT male samples, except in *. By contrast, none of the *Mecp2*-null males produce *darcin*. In addition, the band corresponding to MUPs is visibly narrower in *Mecp2*-null males than in WT, suggesting a general deficit in masculine, testosterone-dependent, release of urinary pheromones. B. Plot profile (yellow line) through individual samples of WT urine (black lines) and *Mecp2*-null urine (blue lines) shows that the intensity and the width of bands corresponding to MUPs is reduced in *Mecp2*-null mice and *darcin* is absent.

Figure 8. Behavioural parameters analysed in the resident animals during the RI-test. First, we analysed aggressive behaviours (A), chemoinvestigation (B) and self-grooming (C) in the residents of the WT_r vs WT_i (black bars) and *Mecp2*-$null_r$ vs WT_i (dotted bars) conditions, and then we analysed the same parameters in the residents of WT_r vs WT_i (black bars) and WT_r vs *Mecp2*-$null_i$ (dotted bars). A) Time spent in attacking/chasing the intruder did not show any significant differences between the groups. However, it can be seen in the bar chart that none of the *Mecp2*-$null_r$ engaged in aggressive interactions during the test. B) Time devoted to chemoinvestigation of the intruder was significantly lower in Mecp2-$null_r$ as compared to WT_r encountering a WT_i. By contrast, this parameter was significantly higher in cases in which the WT_r was presented with a *Mecp2*-$null_i$ C) Self-grooming was significantly higher in *Mecp2*-$null_r$ as compared to WT_r. Values are presented as mean ± SEM. *p<0.05, **p<0.01

Figure 9. Habituation-dishabituation test revealed that *Mecp2*-null males are not anosmic, but display reduced olfactory investigation. A) Complete curve of exploration of the cotton-swab impregnated with

water, male urine and rose odour in WT (filled dots) and *Mecp2*-null males (empty dots). There were no significant differences in time spent investigating the cotton-swab, except for time investigating the first presentation of rose odour. B) Total exploration time during the test was significantly decreased in Mecp2-null males (white bars) as compared to WT (black bars). C) Discrimination index was different from zero in animals of both genotypes (i.e. they were not anosmic), but it was significantly higher in WT as compared to *Mecp2*-null males. Values are presented as mean ± SEM. *p<0.05, **p<0.01, comparisons WT vs *Mecp2*-null; +p>0.05, ++p>0.01, comparison of DI against 0.

Figure 10. Data from social interaction test. A) Time spent investigating a stranger mouse was significantly different from time spent investigating an empty compartment in both WT (black bars) and *Mecp2*-null males (white bars). However, *Mecp2*-null males showed higher exploration of the stranger mice than WT did. B) *Mecp2*-null males displayed enhanced preference for a stranger mouse in the social recognition test. Values are presented as mean ± SEM. **p<0.01, ***p<0.01, comparisons between stimuli; +p>0.05, ++p>0.01, comparisons between genotypes.

Figure

Click here to access/download;Figure;Fig._1.tif

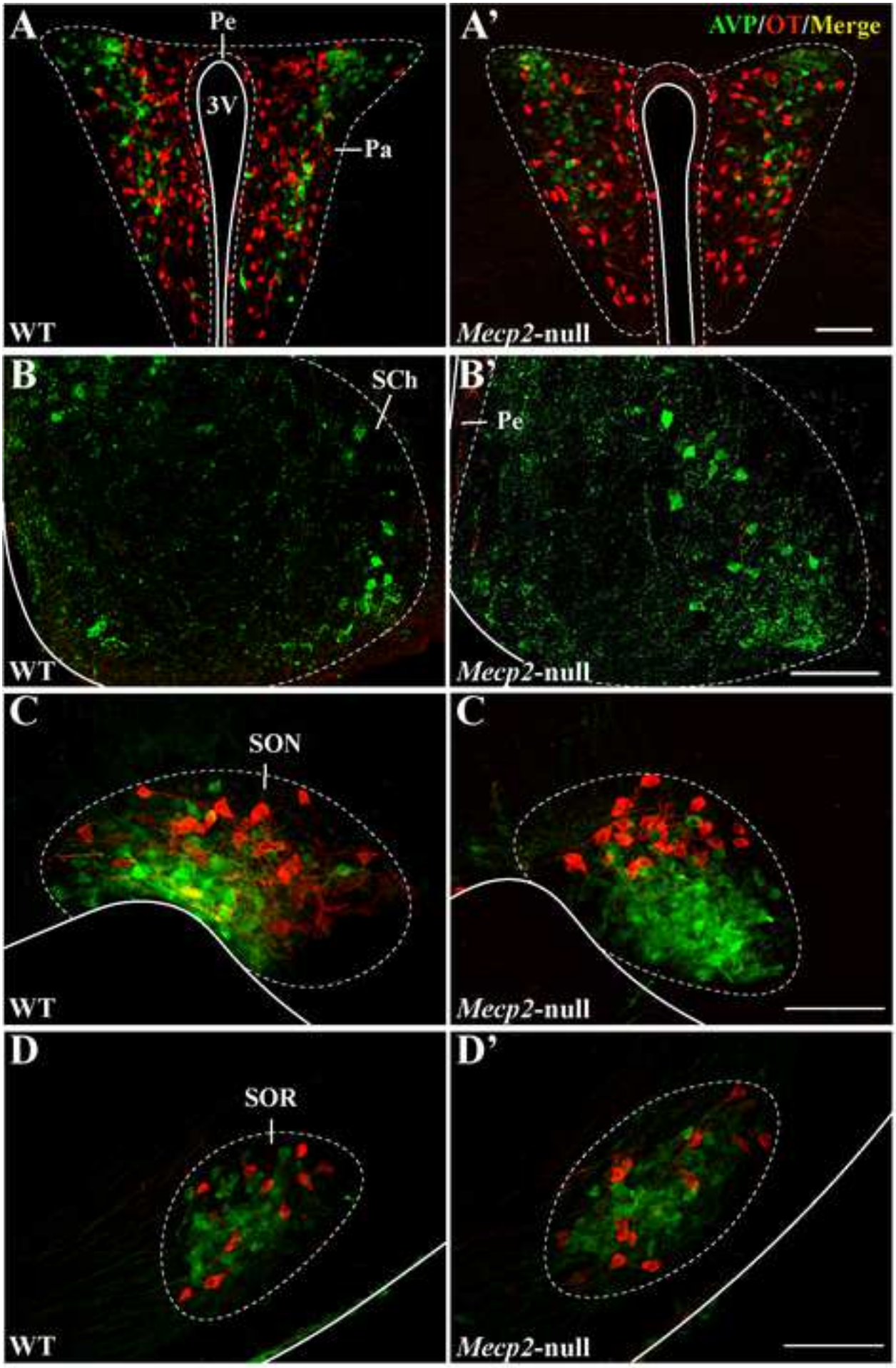

Figure

Click here to access/download;Figure;Fig._2.tif

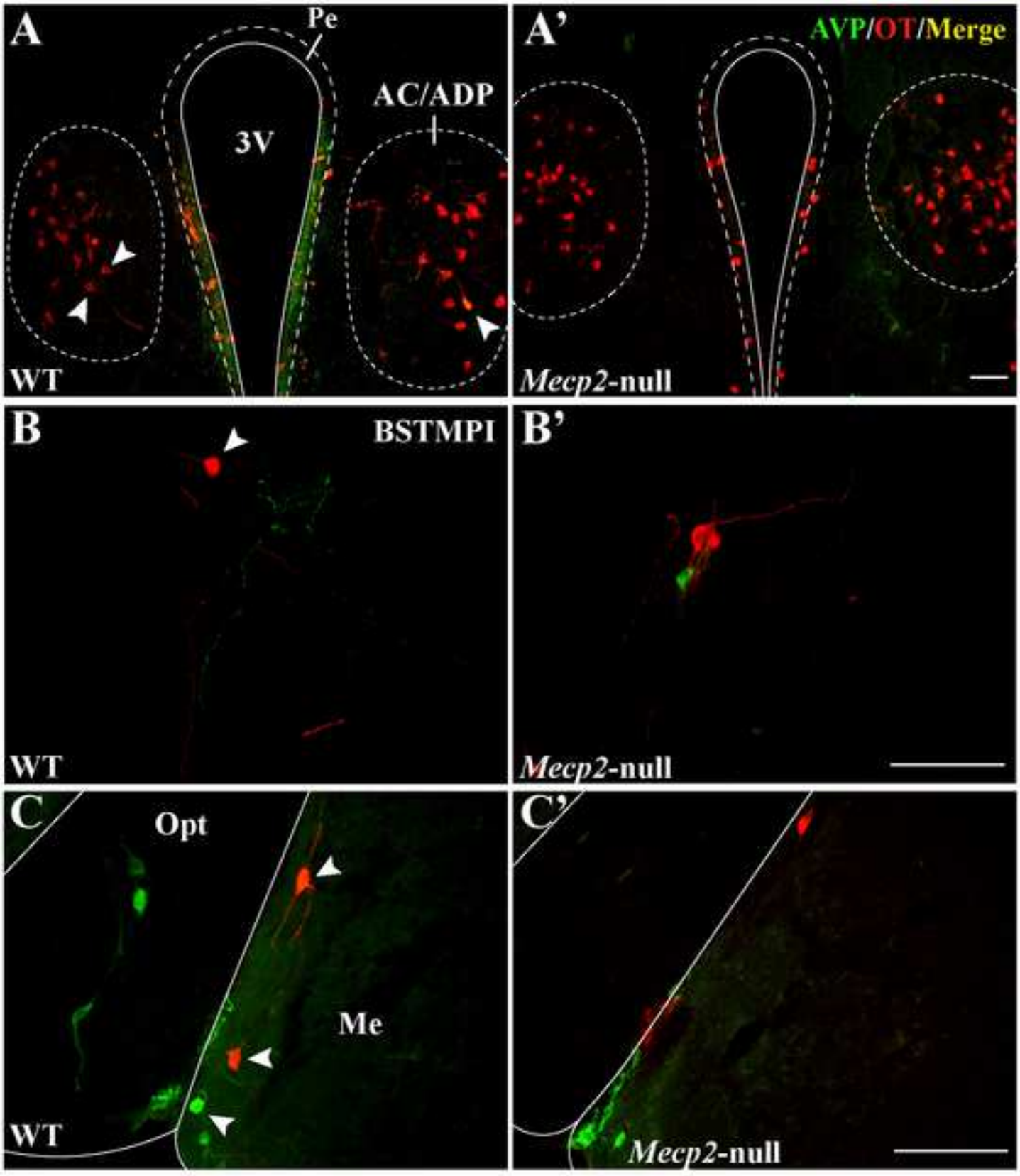

Figure

Click here to access/download;Figure;Fig._3.tif

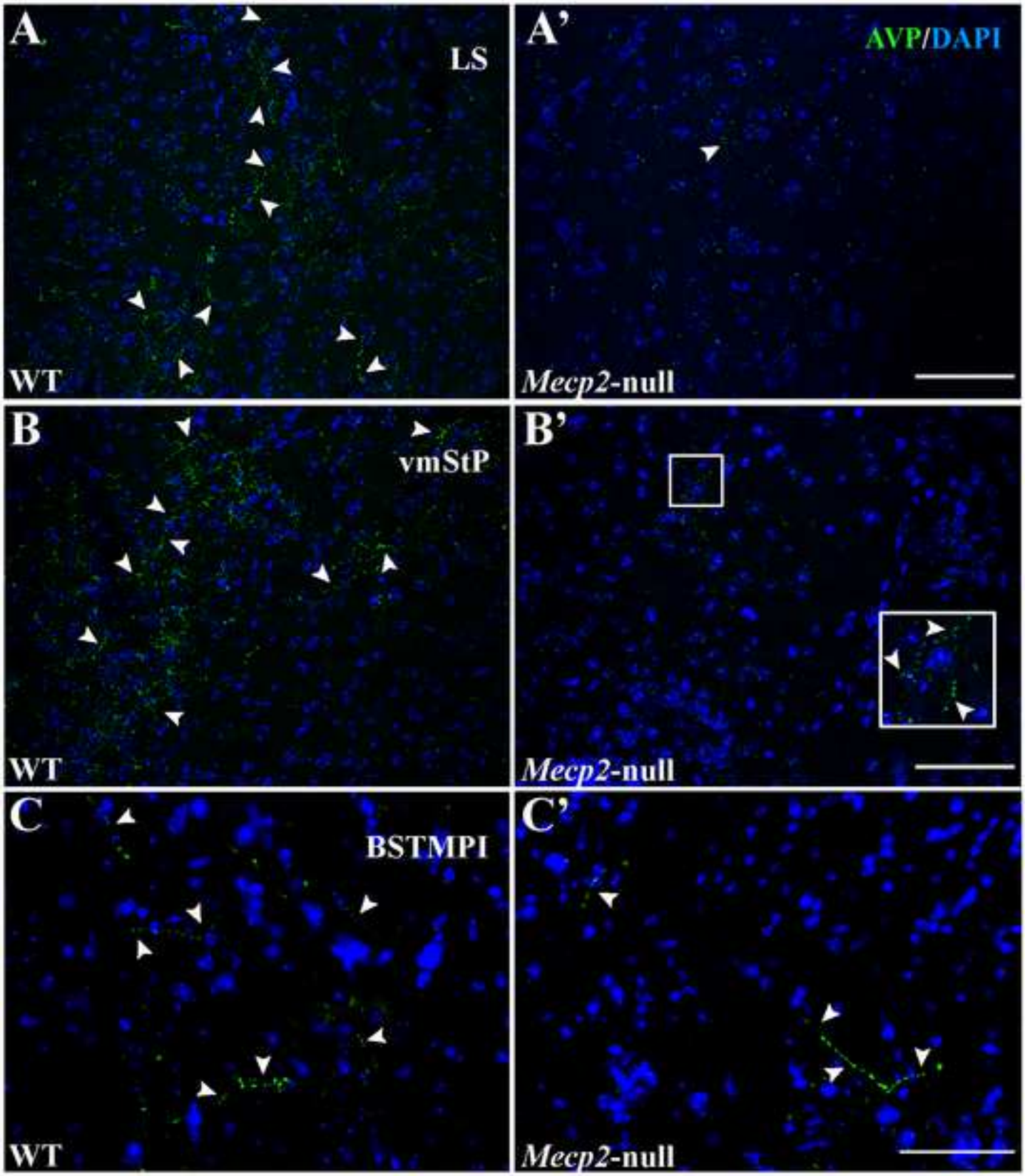

Figure

Click here to access/download;Figure;Fig._4.tif

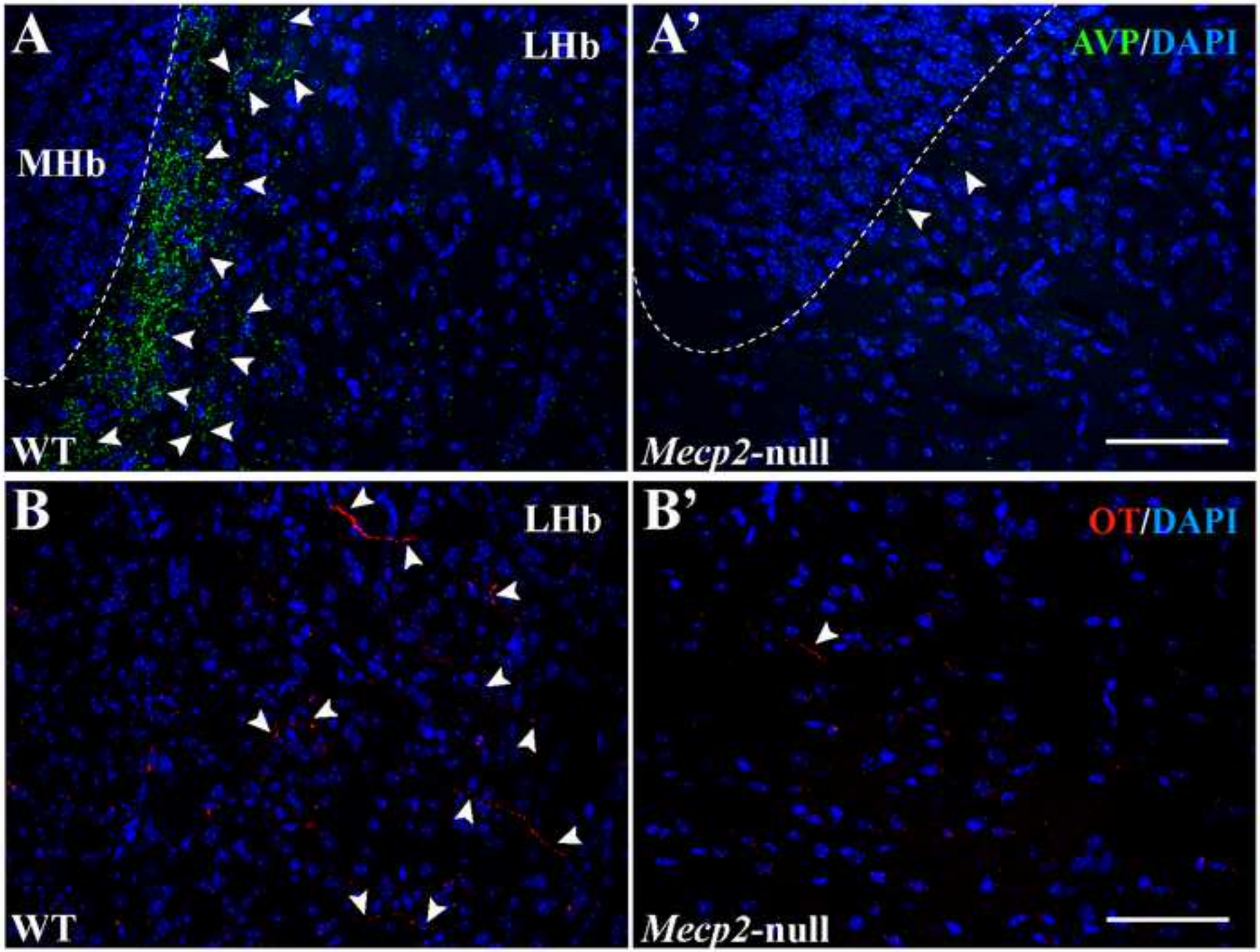

Figure

Click here to access/download;Figure;Fig._5.tiff

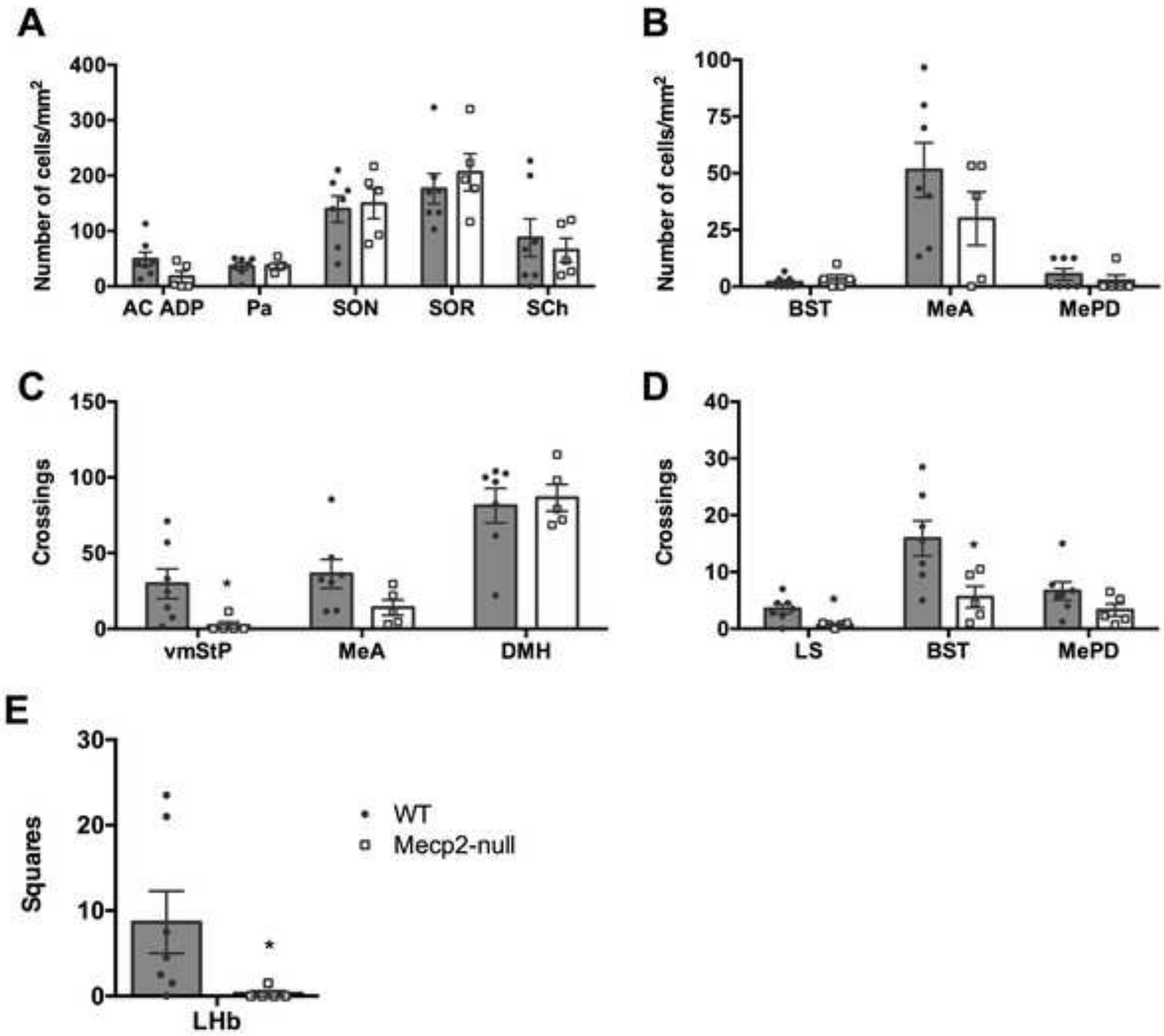

Figure

Click here to access/download;Figure;Fig._6.tiff

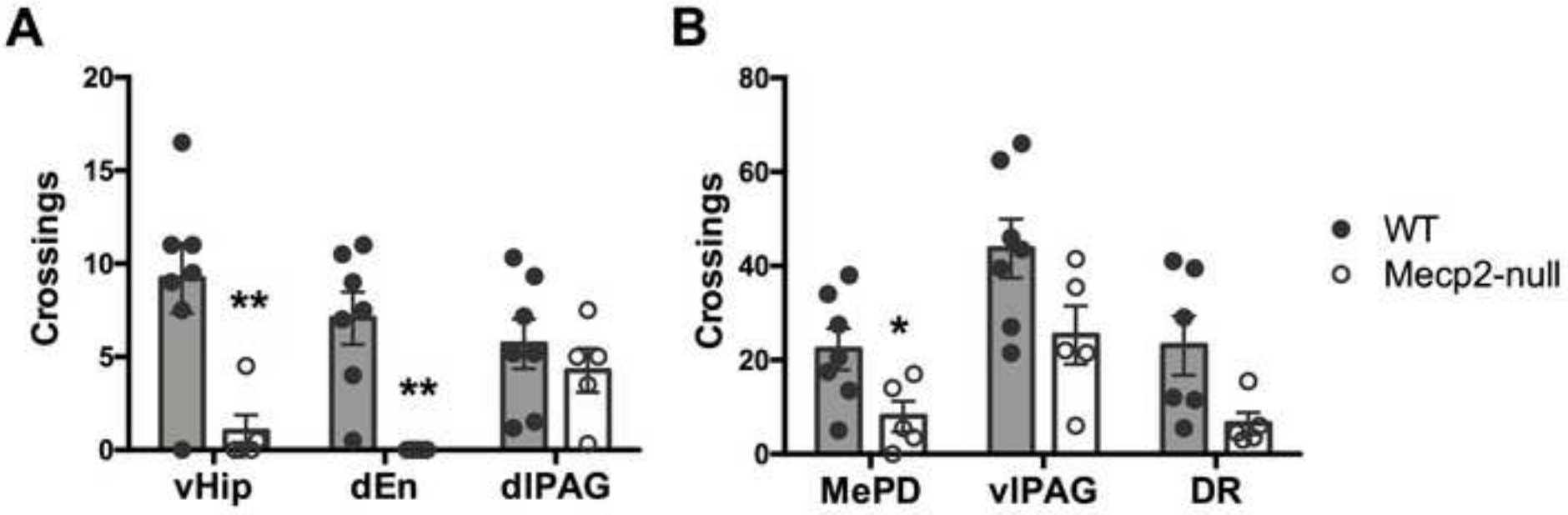

Figure

Click here to access/download;Figure;Fig._7.tif

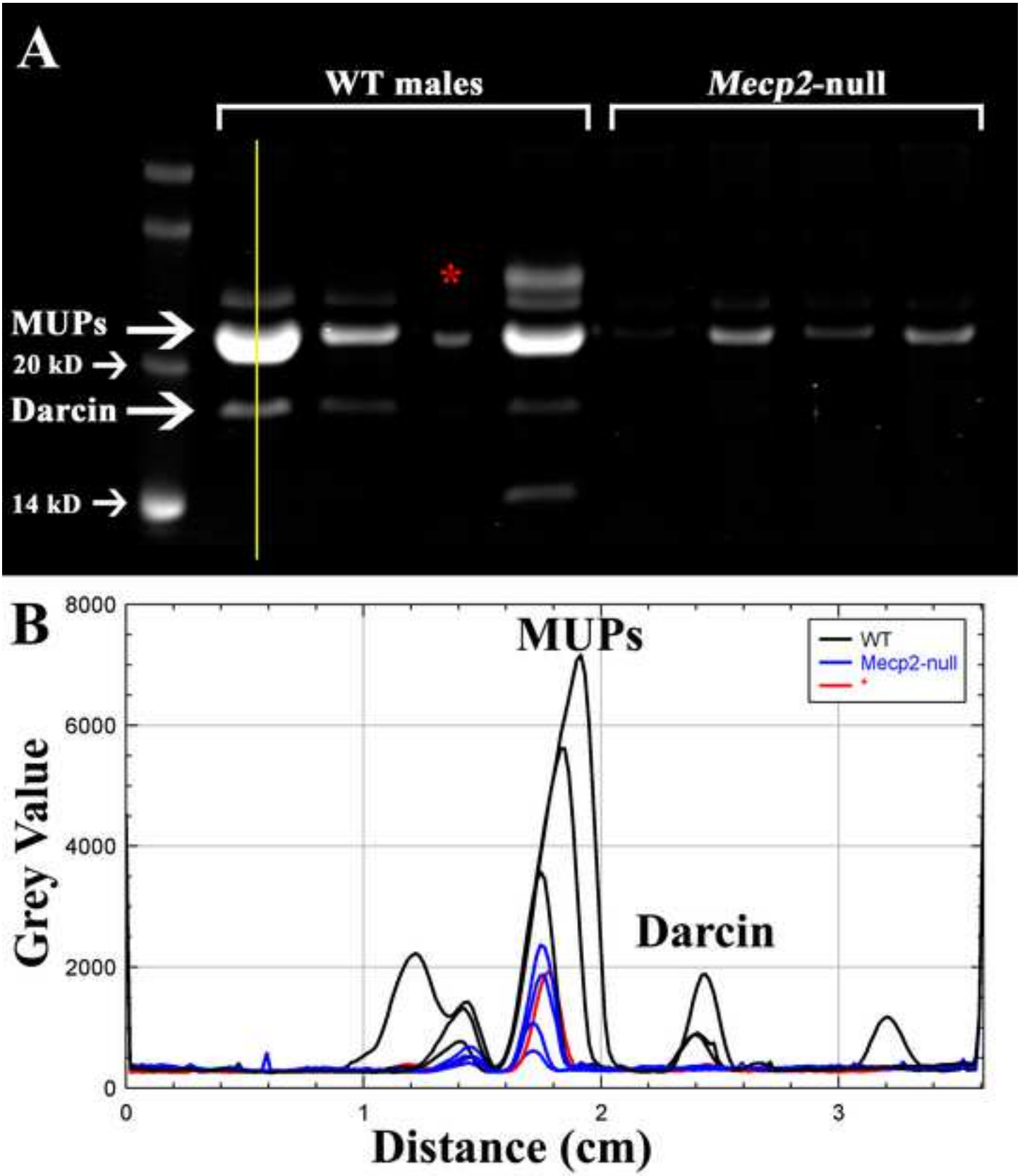

Click here to access/download;Figure;Fig._8.tiff

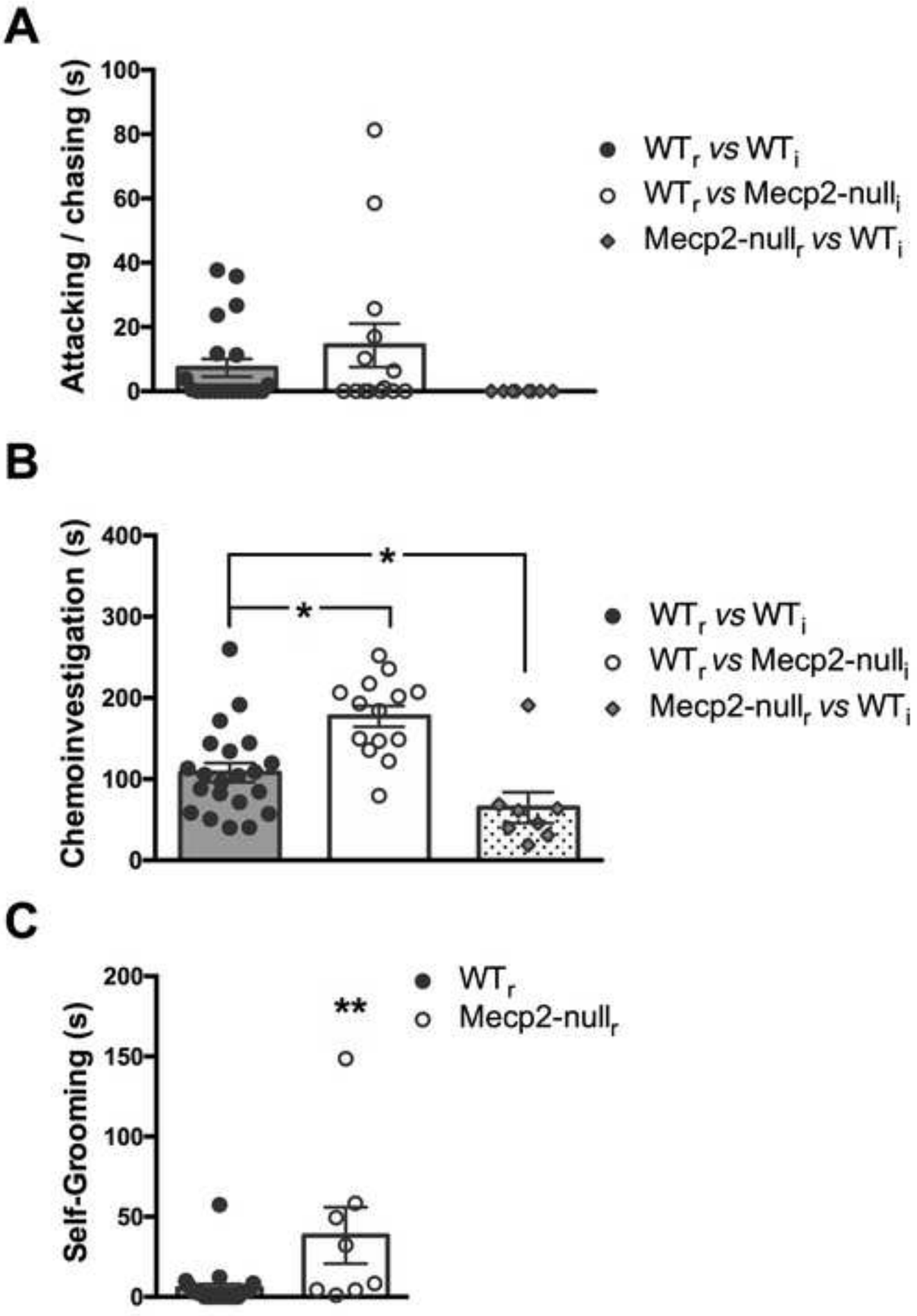

Figure

Click here to access/download;Figure;Fig._9.tiff

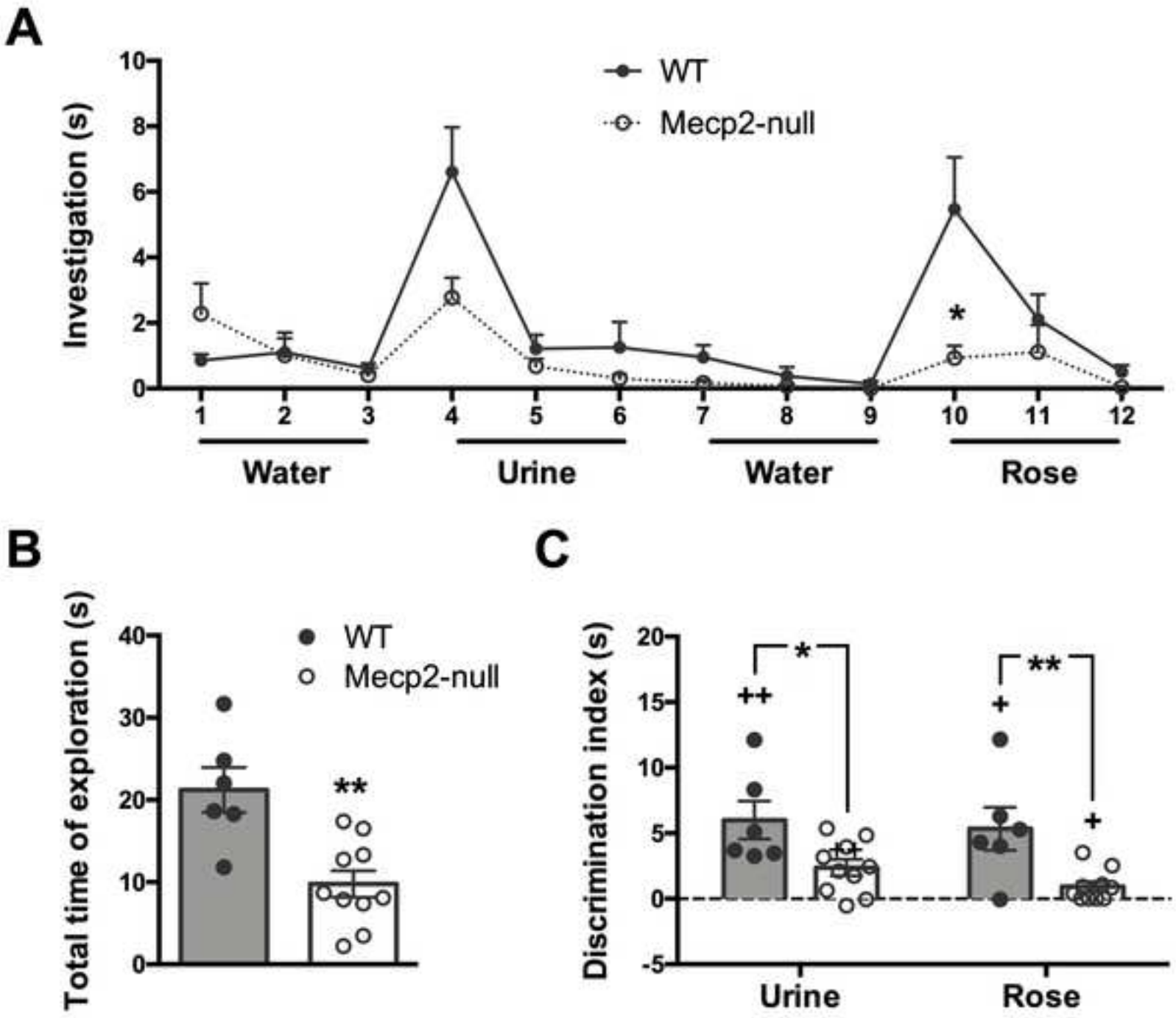

Figure

Click here to access/download;Figure;Fig._10.tiff

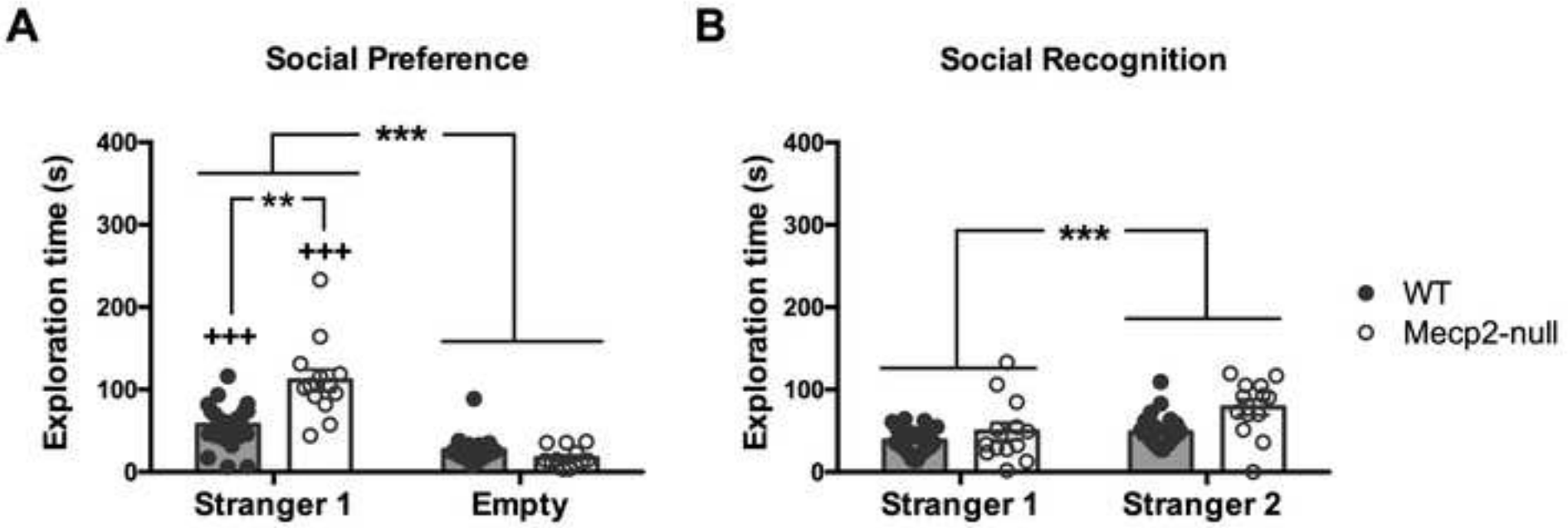

Table

Table 1. Nuclei and Bregma levels (following Paxinos & Franklin, 2012) selected for quantification of AVP and OT in *Mecp2*-mutant and WT mice.

Nucleus	AVP	OT	Bregma level (mm)
dEn	Fibres	-	-2.92
vHip	Fibres	-	-2.92
AcbC	-	Fibres	+1.10
AcbSh	-	Fibres	+1.18, +1.10, +0.98
vmStP	Fibres	Fibres	+1.10
LS	Fibres	Fibres	+0.38, +0.14
BSTMPI	Fibres, somata	Fibres, somata	-0.22
MeA	Fibres, somata	Fibres, somata	-1.22
MePD	Fibres, somata	Fibres, somata	-1.34
Ce	-	Fibres	-1.34
LHb	Fibres	Fibres	-1.46
AC/ADP	Somata	Somata	-0.22
Pa	Somata	Somata	-0.58, -0.70, -0.94
SCh	Somata	-	-0.82
SON	Somata	Somata	-0.82
SOR	Somata	Somata	-1.34
DMH	Fibres	Fibres	-1.46
dlPAG	Fibres	-	-4.24, -4.48, -4.72
vlPAG	Fibres	Fibres	-4.24, -4.48, -4.72
DR	Fibres	-	-4.72

Table 2: Quantitative analysis of average AVP and OT-ergic somata/mm^2 in different brain nuclei of *Mecp2*-het females and their WT siblings. Values are presented as mean ± SEM. We did not find statistically significant differences between genotypes in any of the brain nuclei analysed. Abbreviations: AC/ADP: nucleus of the anterior commissure / anterodorsal preoptic nucleus; BSTMPI: bed nucleus of the stria terminalis, medial division, posterointermediate part; MeA: medial amygdaloid nucleus, anterior part; MePD: medial amygdaloid nucleus, posterodorsal part; Pa: paraventricular hypothalamic nucleus; SCh: suprachiasmatic nucleus; SON: supraoptic nucleus.

	AVP-ir cells/mm^2		**OT-ir cells/mm^2**	
	WT	***Mecp2*-het**	**WT**	***Mecp2*-het**
AC/ADP	25.33 ± 13.89	8 ± 3.89	146.67 ± 49.98	162 ± 50.86
BSTMPI	0 ± 0	0.56 ± 0.61	9.33 ± 3.06	9.44 ± 1.74
MeA	5 ± 2.85	5.33 ± 3.74	7.5 ± 1.43	3.33 ± 1.05
MePD	0 ± 0	2.5 ± 2.5	5 ± 5	2.08 ± 2.28
Pa	13.99 ± 4.54	12.26 ± 2.53	59.74 ± 6.01	70.95 ± 4.15
SCh	38.67 ±22.45	10.67 ± 4.52	-	-
SON	52 ± 10.73	50.56 ± 10.35	138 ± 19.54	130.56 ± 21.67

Table 3: Quantitative analysis of AVP and OT-ergic innervation in different nuclei of *Mecp2*-het females and their WT controls. Values are presented as mean ± SEM. We did not find statistically significant differences between genotypes in any of the brain nuclei analysed. Abbreviations: AcbC: nucleus accumbens, core; AcbSh: nucleus accumbens, shell; BSTMPI: bed nucleus of the stria terminalis, medial division, posterointermediate part; Ce: central amygdaloid nucleus; DMH: dorsomedial hypothalamic nucleus; DR: dorsal raphe nucleus; LHb: lateral habenular nucleus; LS: lateral septum; MeA: medial amygdaloid nucleus, anterior part; MePD: medial amygdaloid nucleus, posterodorsal part; vlPAG: ventrolateral periaqueductal grey; vmStP: ventromedial striatopallidum.

	AVP-ir crossing fibres		**OT-ir crossing fibres**	
	WT	***Mecp2*-het**	**WT**	***Mecp2*-het**
AcbC	-	-	18.10 ± 2.4	13.1 ± 0.93
AcbSh	-	-	5.6 ± 1.39	11.7 ± 2.93
BSTMPI	2.3 ± 0.97	2.42 ± 1.36	57.9 ± 4.94	54.67 ± 10.18
Ce			19.4 ± 4.3	9.83 ± 3.18
DMH	44.2 ± 13.68	29 ± 11.67	101.5 ± 24.84	74 ± 17.94
DR	-	-	28.8 ± 3.09	34.67 ± 7.82
LHb	-	-	1.1 ± 0.58	0.08 ± 0.08
LS	0.25 ± 0.11	0.25 ± 0.11	9.65 ± 1.73	11.8 ± 1.65
MeA	8.38 ± 4.54	11.6 ± 2.59	17.13 ± 2.81	18 ± 4.62
MePD	1 ± 0.73	1.85 ± 1.44	11 ± 2.5	10.22 ± 1.58
vlPAG	-	-	32 ± 5.64	46.58 ± 10.96
vmStP	2.3 ± 2.3	0 ± 0	10.4 ± 3.04	4.6 ± 1.6

Table 4: Quantitative analysis of OT-ergic innervation in different nuclei of *Mecp2*-null males and their WT controls. Values are presented as mean ± SEM. We did not find statistically significant differences between genotypes in any of the brain nuclei analysed except for lateral habenula. Abbreviations: AcbC: nucleus accumbens, core; AcbSh: nucleus accumbens, shell; BSTMPI: bed nucleus of the stria terminalis, medial division, posterointermediate part; Ce: central amygdaloid nucleus; DMH: dorsomedial hypothalamic nucleus; DR: dorsal raphe nucleus; LHb: lateral habenular nucleus; LS: lateral septum; MeA: medial amygdaloid nucleus, anterior part; MePD: medial amygdaloid nucleus, posterodorsal part; vlPAG: ventrolateral periaqueductal grey; vmStP: ventromedial striatopallidum.

	OT-ir crossing fibres	
	WT	***Mecp2*-null**
AcbC	24.21 ± 6.33	21 ± 5.68
AcbSh	9.64 ± 2.06	4.4± 1.66
BSTMPI	67.29 ± 5.29	47.3 ± 11.98
Ce	33.79 ± 6.74	20.3 ± 3.60
DMH	121.71 ± 13.11	96.4 ± 14.16
DR	42 ± 12.6	41 ± 8.2
LHb	1.29 ± 0.32	0 ± 0**
LS	12.96 ± 1.12	11.45 ± 2.13
MeA	39.64 ± 7.39	20.9 ± 6.53
MePD	14.86 ± 1.20	15.55 ± 2.22
vlPAG	50.43 ± 15.12	39.50 ± 8.95
vmStP	13.79 ± 1.78	12.60 ± 2.65

Click here to access/download
Electronic Supplementary Material
renamed_79eed.pdf